Publish Date:
December 2017
Volume 3, Issue 6

JSHD

Journal of Structural Heart Disease

OFFICIAL JOURNAL OF THE PICS FOUNDATION

PICS Foundation

PEDIATRIC AND ADULT INTERVENTIONAL CARDIAC SYMPOSIUM

Published by
Science International Corp.
ISSN 2325-4637

Now accepting papers at http://structuralheartdisease.org

Committed to Advancing Transcatheter Heart Valve Therapy

Edwards SAPIEN XT Transcatheter Heart Valve

Approved for Pulmonic Procedures

The SAPIEN XT valve is approved for pulmonic procedures in pediatric and adult patients with a dysfunctional, non-compliant right ventricular outflow tract (RVOT) conduit.

SAPIEN XT Valve Sizing—Pulmonic

23 mm	26 mm	29 mm
20-23 mm	23-26 mm	26-29 mm

Diameter of intended location within the conduit

Edwards Lifesciences is driving the innovation, collaboration, and education needed to bring transcatheter technology to more patients worldwide.

» Visit **Edwards.com/pulmonic** for more information

See adjacent page for Important Safety Information.

CAUTION: Federal (United States) law restricts this device to sale by or on the order of a physician.

Edwards Lifesciences • One Edwards Way, Irvine CA 92614 USA • edwards.com

Edwards

Important Safety Information

EDWARDS SAPIEN XT TRANSCATHETER HEART VALVE WITH THE NOVAFLEX+ DELIVERY SYSTEM – PULMONIC

Indications: The Edwards SAPIEN XT transcatheter heart valve (THV) systems are indicated for use in pediatric and adult patients with a dysfunctional, non-compliant right ventricular outflow tract (RVOT) conduit with a clinical indication for intervention and: pulmonary regurgitation ≥ moderate and/or mean RVOT gradient ≥ 35 mmHg.

Contraindications: The THV and delivery systems are contraindicated in patients with inability to tolerate an anticoagulation/antiplatelet regimen or who have active bacterial endocarditis.

Warnings: The devices are designed, intended, and distributed for single use only. **Do not resterilize or reuse the devices.** There are no data to support the sterility, nonpyrogenicity, and functionality of the devices after reprocessing. Assessment for coronary compression risk prior to valve implantation is essential to prevent the risk of severe patient harm. Incorrect sizing of the THV may lead to paravalvular leak, migration, embolization and/or RVOT rupture. Accelerated deterioration of the THV may occur in patients with an altered calcium metabolism. Prior to delivery, the THV must remain hydrated at all times and cannot be exposed to solutions other than its shipping storage solution and sterile physiologic rinsing solution. THV leaflets mishandled or damaged during any part of the procedure will require replacement of the THV. Do not use the THV if the tamper evident seal is broken, the storage solution does not completely cover the THV, the temperature indicator has been activated, the THV is damaged, or the expiration date has elapsed. Do not mishandle the NovaFlex+ delivery system or use it if the packaging or any components are not sterile, have been opened or are damaged (e.g. kinked or stretched), or the expiration date has elapsed. Use of excessive contrast media may lead to renal failure. Measure the patient's creatinine level prior to the procedure. Contrast media usage should be monitored. Patient injury could occur if the delivery system is not un-flexed prior to removal. Care should be exercised in patients with hypersensitivities to cobalt, nickel, chromium, molybdenum, titanium, manganese, silicon, and/or polymeric materials. The procedure should be conducted under fluoroscopic guidance. Some fluoroscopically guided procedures are associated with a risk of radiation injury to the skin. These injuries may be painful, disfiguring, and long-lasting. THV recipients should be maintained on anticoagulant/antiplatelet therapy as determined by their physician. This device has not been tested for use without anticoagulation. Do not add or apply antibiotics to the storage solution, rinse solutions, or to the THV.

Precautions: Safety, effectiveness, and durability of the THV have not been established for implantation within a previously placed surgical or transcatheter pulmonic valve. Long-term durability has not been established for the THV. Regular medical follow-up is advised to evaluate THV performance. Glutaraldehyde may cause irritation of the skin, eyes, nose and throat. Avoid prolonged or repeated exposure to, or breathing of, the solution. Use only with adequate ventilation. If skin contact occurs, immediately flush the affected area with water; in the event of contact with eyes, immediately flush the affected area with water and seek immediate medical attention. For more information about glutaraldehyde exposure, refer to the Material Safety Data Sheet available from Edwards Lifesciences. Patient anatomy should be evaluated to prevent the risk of access that would preclude the delivery and deployment of the device. To maintain proper valve leaflet coaptation, do not overinflate the deployment balloon. Appropriate antibiotic prophylaxis is recommended post-procedure in patients at risk for prosthetic valve infection and endocarditis. Safety and effectiveness have not been established for patients with the following characteristics/comorbidities: Echocardiographic evidence of intracardiac mass, thrombus, or vegetation; a known hypersensitivity or contraindication to aspirin, heparin or sensitivity to contrast media, which cannot be adequately premedicated; pregnancy; and patients under the age of 10 years.

Potential Adverse Events: Potential risks associated with the overall procedure including potential access complications associated with standard cardiac catheterization, balloon valvuloplasty, the potential risks of conscious sedation and/or general anesthesia, and the use of angiography: death; respiratory insufficiency or respiratory failure; hemorrhage requiring transfusion or intervention; cardiovascular injury including perforation or dissection of vessels, ventricle, myocardium or valvular structures that may require intervention; pericardial effusion or cardiac tamponade; embolization including air, calcific valve material or thrombus; infection including septicemia and endocarditis; heart failure; myocardial infarction; renal insufficiency or renal failure; conduction system defect arrhythmia; arteriovenous fistula; reoperation or reintervention; ischemia or nerve injury; pulmonary edema; pleural effusion, bleeding; anemia; abnormal lab values (including electrolyte imbalance); hypertension or hypotension; allergic reaction to anesthesia, contrast media, or device materials; hematoma or ecchymosis; syncope; pain or changes at the access site; exercise intolerance or weakness; inflammation; angina; fever. Additional potential risks associated with the use of the THV, delivery system, and/or accessories include: cardiac arrest; cardiogenic shock; emergency cardiac surgery; coronary flow obstruction/transvalvular flow disturbance; device thrombosis requiring intervention; valve thrombosis; device embolization; device malposition requiring intervention; valve deployment in unintended location; structural valve deterioration (wear, fracture, calcification, leaflet tear/tearing from the stent posts, leaflet retraction, suture line disruption of components of a prosthetic valve, thickening, stenosis); paravalvular or transvalvular leak; valve regurgitation; hemolysis; device explants; nonstructural dysfunction; and mechanical failure of delivery system, and/or accessories.

Edwards Crimper

Indications: The Edwards crimper is indicated for use in preparing the Edwards SAPIEN XT transcatheter heart valve for implantation.

Contraindications: No known contraindications.

Warnings: The device is designed, intended, and distributed for single use only. **Do not resterilize or reuse the device.** There are no data to support the sterility, nonpyrogenicity, and functionality of the device after reprocessing. Do not mishandle the device. Do not use the device if the packaging or any components are not sterile, have been opened or are damaged, or the expiration date has elapsed.

Precautions: For special considerations associated with the use of this device prior to THV implantation, refer to the SAPIEN XT transcatheter heart valve Instructions for Use.

Potential Adverse Events: No known potential adverse events.

CAUTION: Federal (United States) law restricts this device to sale by or on the order of a physician.

Edwards Lifesciences • One Edwards Way, Irvine CA 92614 USA • edwards.com

Edwards

NOW ENROLLING:

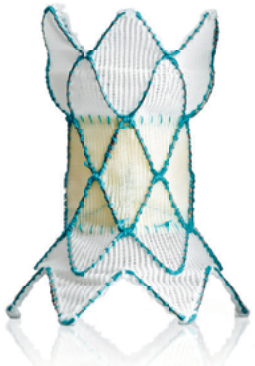

Harmony™ Transcatheter Pulmonary Valve (TPV) Clinical Study

WHAT IS THE MEDTRONIC HARMONY TPV CLINICAL STUDY?

The study is a multi-center prospective, non-randomized, interventional pre-market study in the United States. The purpose of the study is to evaluate the safety and effectiveness of the Harmony TPV system in patients who have congenital heart disease and are clinically indicated for pulmonary valve replacement. The trial will involve up to 40 subjects implanted at 10 study centers.

WHO CAN PARTICIPATE?

Patients who have pulmonary regurgitation:

- Severe pulmonary regurgitation by echocardiography, or
- Pulmonary regurgitant fraction ≥ 30% by cardiac magnetic resonance imaging

Patients who have a clinical indication for surgical placement of a RV-PA conduit or prosthetic pulmonary valve:

- Subject is symptomatic secondary to pulmonary insufficiency (e.g., exercise intolerance, fluid overload), or
- Right ventricular end diastolic volume index ≥ 150 mL/m^2, or
- Subject has RVEDV:LVEDV Ratio ≥ 2.0

HOW CAN I LEARN MORE ABOUT THE HARMONY TPV CLINICAL STUDY?

For additional information about the program, please contact Medtronic at:
RS.HarmonyTPVClinicalStudy@medtronic.com

CAUTION: Investigational Device. Limited by Federal Law (USA) to Investigational Use.

medtronic.com

710 Medtronic Parkway
Minneapolis, MN 55432-5604
USA
Tel: (763) 514-4000
Fax: (763) 514-4879
Toll-free: (800) 328-2518

LifeLine
CardioVascular Technical Support
Tel: (877) 526-7890
Tel: (763) 526-7890
Fax: (763) 526-7888
rs.cstechsupport@medtronic.com

UC201711884 EN 04/2017

Medtronic

Editorial Board

James Hermiller — The Care Group (Indianapolis, IN)

Howard Herrmann — University of Pennsylvania (Philadelphia, PA)

David Holmes — Mayo Clinic (Rochester, MN)

Noa Holoshitz — Rush University Medical Center (Chicago, IL)

Ralf Holzer — Sidra Medical & Research Center (Doha, Qatar)

Eric Horlick — University of Toronto (Toronto, Canada)

Reda Ibrahim — Montreal Heart Institute (Montreal, Canada)

Michel Ilbawi — Rush University Medical Center (Chicago, IL)

Frank Ing — LA Children's Hospital (Los Angeles, CA)

Alexander Javois — Hope Children's Hospital (Oak Lawn, IL)

Thomas Jones — Seattle Children's Hospital (Seattle, WA)

Saibal Kar — Cedars Sinai Medical Center (Los Angeles, CA)

Clifford Kavinsky — Rush University Medical Center (Chicago, IL)

Joseph Kay — University of Colorado (Denver, CO)

Damien Kenny — Rush University Medical Center (Chicago, IL)

Morton Kern — University of California Irvine (Irvine, CA)

Michael Kim — University of Colorado (Aurora, CO)

Seong-Ho Kim — Cheju Halla General Hospital (South Korea)

Susheel Kodali — Columbia University Medical Center (New York, NY)

Jackie Kreutzer — Pittsburgh Children's Hospital (Pittsburgh, PA)

Shelby Kutty — Children's Hospital and University of Nebraska Medical Center (Omaha, NB)

Bray Patrick-Lake — PFO Research Foundation (Boulder, CO)

Michael Landzberg — Boston Children's Hospital (Boston, MA)

Geoffrey Lane — Royal Melbourne Hospital (Melbourne, Australia)

Roberto Lang — University of Chicago Medical Center (Chicago, IL)

John Lasala — Barnes Jewish Hospital, Washington University (St. Louis, MO)

Martin B. Leon — Columbia University (New York, NY)

Daniel Levi — UCLA Medical Center (Los Angeles, CA)

Scott Lim — University of Virginia Health System (Charlottesville, VA)

Michael Mack — Baylor Healthcare System (Plano, TX)

Francesco Maisano — University of Zurich (Zurich, Switzerland)

Raj Makkar — Cedars Sinai Medical Center (Los Angeles, CA)

Robert March — Rush University Medical Center (Chicago, IL)

Gwen Mayes — VP National Patient Advocate Foundation (Washington, DC)

Pat McCarthy — Northwestern Memorial Hospital (Chicago, IL)

Doff McElhinney — New York University (New York, NY)

John Messenger — University of Colorado (Denver, CO)

Friedrich Mohr — Herzzentrum Universitaet Leipzig (Leipzig, Germany)

Tarek Momenah — Prince Salman Cardiac Center (Riyadh, Saudi Arabia)

Issam Moussa — (Jacksonville, FL)

Michael Mullen — The Heart Hospital (London, England)

David Muller — St. Vincent's Hospital (Sydney, Australia)

William O'Neill — Henry Ford Hospital (Detroit, MI)

Igor Palacios — Mass General Hospital (Boston, MA)

SJ Park — University of Ulsan College of Medicine (Seoul, Korea)

Carlos Pedra — Danta Pazzanese Instituto de Cardiologia (Sao Paolo, Brazil)

Alejandro Peirone — Children's Hospital of Cordoba (Cordoba, Argentina)

Giacomo Pongiglione — Bambino Gesu Hospital (Rome, Italy)

Matthew Price — Scripps Clinic (La Jolla, CA)

Robert Quaife — University of Colorado (Denver, CO)

Shakeel Qureshi — Evelina Children's Hospital (London, UK)

Steve Ramee — Oschner Clinic (New Orleans, LA)

Mark Reisman	Swedish Medical Center (Seattle, WA)
John Rhodes	Miami Children's Hopsital (Miami, FL)
Charanjit Rihal	Mayo Clinic (Rochester, MN)
Richard Ringel	Johns Hopkins Medical Center (Baltimore, MD)
Carlos Ruiz	Lenox Hill Hospital (New York, NY)
Ernesto Salcedo	University of Colorado (Denver, CO)
Joachim Schofer	Hamburg University Cardiovascular Center (Hamburg, Germany)
Paul Sorajja	Minneapolis Heart Institute Foundation (Minneapolis, MN)
Christian Spies	Queen's Heart Physician Practice (Honolulu, HI)
Frank Silvestry	University of Pennsylvania Hospital (Philadelphia, PA)
Gregg Stone	Columbia University (New York, NY)
Corrado Tamborino	University of Catania (Catania, Italy)
Vinod Thourani	Emory University (Atlanta, GA)
Jonathan Tobis	UCLA Medical Center (Los Angeles, CA)
Murat Tuczu	Cleveland Clinic Foundation (Cleveland, OH)
Zoltan Turi	Robert Wood Johnson Medical School (Camden, NJ)
Alec Vahanian	Bichat University Hospital (Paris, France)
Joseph J. Vettukattil	Spectrum Health (Grand Rapids, MI)
Kevin Walsh	Our Lady's Hospital (Dublin, Ireland)
John Webb	St. Paul Hospital Vancouver (British Columbia, Canada)
Brian Whisenant	Intermountain Medical Center (Salt Lake City, Utah)
Matthew Williams	Mount Sinai Medical Center (New York, NY)
Neil Wilson	University of Colorado (Denver, CO)
Evan Zahn	Cedars Sinai Medical Center (Los Angeles, CA)

JSHD
Journal of Structural Heart Disease

Volume 3, Issue 6, December 2017

Journal of Structural Heart Disease (ISSN 2325-4637) is an online open-access journal issued bi-monthly (6 issues per year, one volume per year) by Science International Corporation.

All correspondence should be directed to: Ziyad M. Hijazi, MD, Editor-in-Chief, Journal of Structural Heart Disease, PO Box 26999, Doha, Qatar. Tel.: +974-4003-6601, E-Mail: jshd@scienceinternational.org

JSHD
Journal of Structural Heart Disease

Original Research Article

Journal of Structural Heart Disease, December 2017, Volume 3, Issue 6:165-175
DOI: https://doi.org/10.12945/j.jshd.2017.030.17

Received: June 26, 2017
Accepted: July 04, 2017
Published online: December 2017

Intentional Fracture of Previously Placed Stents: Impact of Pre-stenting in a Piglet Model

András Bratincsák, MD, PhD[1], William Van Alstine, DVM, PhD, DACVP[3], Lindsay Koren, BE[2], Kimberly Stoughton, CVT[3], José Negrón-Garcia, CVT[3], Anthony Ragheb, PhD[2], Hannah El-Sabrout, HSDG[4], John W. Moore, MD, MPH[5], Howaida el-Said, MD, PhD[5*]

[1] Kapi'olani Medical Center for Women and Children, University of Hawaii, Honolulu, Hawaii, United States

[2] Cook Medical, Bloomington, Indiana, United States

[3] Cook Research Incorporated, West Lafayette, Indiana, United States

[4] Department of Molecular, Cell and Developmental Biology, University of California, Los Angeles, California, United States

[5] Rady Children's Hospital, University of California San Diego, San Diego, California, United States

Abstract

Background: **Intentional stent fracture in vivo induces medial dissection/vessel injury. Spontaneous stent fracture in humans can lead to stent collapse, hemodynamic compromise, and embolization of stent fragments, which could be prevented by pre-stenting.**

Objectives: To evaluate the short-term and mid-term effects of pre-stenting prior to intentional stent fracture on vessel size and integrity in a piglet model.

Methods: **Five months after 14 low-profile stents (Cook Formula 418 stents) were implanted in the aorta of four piglets, they were intentionally fractured using ultra-high-pressure balloons with (pre-stent group) or without (single stent group) with another stent placed inside.**

Results: **Compared with the single stent group, the pre-stent group showed a significantly larger vessel lumen area (109 mm2 (89–141) vs. 57 mm2 (47–73), P = 0.019), less mid-term luminal diameter loss (44% (26–59) vs. 75% (62–85), P = 0.007), lack of strut protrusion, and improved endothelialization (100% (89–100) vs. 73% (56–96), P = 0.022). Vessel wall injury was similar between groups at the time of stent fracture; however, the injury score was significantly improved at mid-term in the pre-stent group compared with the single stent group (P = 0.046). No damage to the external part of the blood vessels or the surrounding soft tissue was noted in either group.**

Conclusion: **Pre-stenting before intentional stent fracture may provide advantages including larger vessel diameter, maintained vessel patency, more complete endothelialization, and lack of stent strut protrusion.**

Key Words

Stent Fracture • Coarctation • Intentional stent fracture

Introduction

Stent implantation in younger patients is facilitated by the availability of low-profile stents that are deliverable through small delivery sheaths, although these smaller stents cannot be dilated to match an adult vessel size [1-3]. Several *in vitro* studies demonstrate that small- and medium-size stents can be fractured using ultra-high-pressure balloons [4, 5]. Recently, an *in vivo* model of stent fracture (i.e., "unzipping") confirmed the feasibility of intentional fracture of several different stents in pigs; however, the report did not mention vessel patency after fracture and admitted to significant vessel injury secondary to intentional fracture, with Cook Formula stents associated with a slightly lower vessel injury score than other stents

Fax +1 203 785 3346
E-Mail: jshd@scienceinternational.org
http://structuralheartdisease.org/

ISSN 2326-4004

Accessible online at:
http://structuralheartdisease.org/

* Corresponding Author:
Howaida el-Said, MD, PhD
Rady Children's Hospital
University of California San Diego
3020 Children's Way, San Diego, CA 92123, USA
Tel. +1 914 409 3091; Fax: +1 858 966 7903; E-Mail: hgelsaid@yahoo.com

Table 1. Group demographics.

	Re-stent group	Single stent group	*p*-value
	n=7	n=7	
Piglet weight (kg)	6.6	8.1	0.0342
Original Stent			
Type	Formula 418	Formula 418	
Stent Size (mm)*			
4	n=3	n=1	
5,6	n=4	n=4	
7,8	n=0	n=2	
Fracture diameter (mm)			
12	n=3	n=1	
16	n=4	n=4	
20	n=0	n=2	
Fracture atm (mean)	14.7 ±4.9	18.4 ±4.8 **	0.1766

* All Formula 418 stents were 12mm in length
** Higher atm for the single stent group can be explained by the fact that the stents were thinner and harder to visualize in the older pig, so more atmospheres were used to insure that they were broken.

and the EV3 stent having the lowest score [6].

Five intentional longitudinal stent fractures were reported in humans using high-pressure balloons without immediate adverse events [7]. *In situ* spontaneous stent fracture in humans is not uncommon and has been reported in up to 21% patients, with resultant obstruction in 80% (of which 39% were considered severe). Some fractures can cause stent collapse, hemodynamic compromise, and embolization of stent fragments, requiring additional intervention in 75% of cases [8, 9]. In a large report of the spontaneous fracture of 3,650 stents, there was a 42% incidence of in-stent restenosis and 4.6% incidence of thrombosis [10]. Furthermore, in a study demonstrating the feasibility of intentional stent fracture in humans, there was a significant incidence of complications (15%), including embolization of stent fragments, unstable stent fracture, vascular tear, non-obstructive intimal tear, and aorto-pulmonary window. All complications except embolization were prevented by pre-stenting [11].

The purpose of the present study was to evaluate the impact of pre-stenting prior to intentional stent fracture in a piglet model.

Methods

Study Design

Experiments were performed using four 6-9-week-old piglets (7–11 kg), in which the aorta at various levels measured 5.7–10 mm. A total of 14 Cook Formula 418 stents (al1 2 mm length) were placed in the four piglets (three stents in two piglets and four stents in two piglets) at a diameter 1–3 mm larger than the vessel size to prevent stent migration. The pigs were allowed to grow for 5 months, during which time the aorta above and below the stent grew to 10.9–22 mm, with the area where the stent was placed being locked at its original size.

In two pigs (one with four stents and the other with three stents), the previously stented area was fractured using ultra-high-pressure Atlas balloons (Bard Peripheral Vascular, Temple, AZ, USA) without pre-stenting (single stent group). The Atlas balloons were over-sized for the region of the stent but matched the size of the adjacent vessel diameter.

In the other two pigs (one with four stents and the other with three stents), the previously stented area was pre-stented prior to stent fracture using Cordis Palmaz Genesis 1910 B peripheral stents (Cordis, Hialeah, FL, USA; pre-stent group). The Genesis stents were mounted on Cordis Powerflex (Cordis, Hialeah, FL, USA) or NuMED BIB (NuMed Inc., Hopkinton, NY, USA) balloon catheters. The Genesis stents were selected for the second set of stents because they are commonly used in the pediatric population and can be ultimately dilated to reach adult vessel size. Balloon size was selected to match the adjacent vessel diameter. Balloon catheters were inflated to their respective recommended maximum pressure to place the Genesis stents inside the smaller Cook Formula stents. High-pressure Atlas balloons were then used to dilate the secondarily placed Genesis stents with simultaneous intentional fracture of the smaller Cook Formula stents.

Two pigs (short-term group; one each from the single stent and pre-stent groups, total of seven stents) were euthanized immediately and the tissue

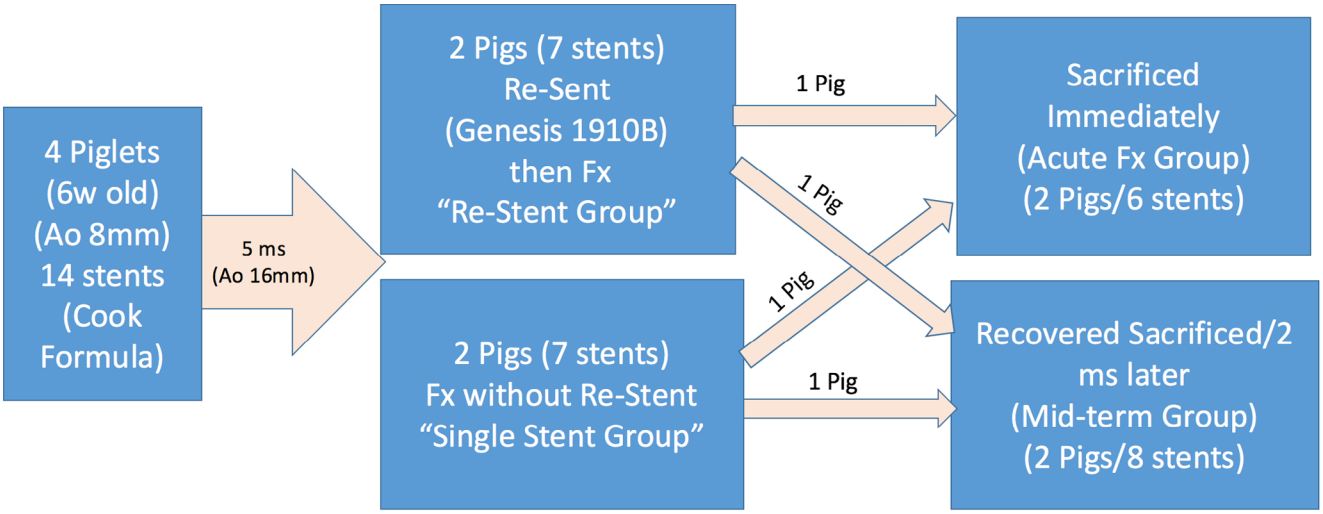

Figure 1. Flow chart showing the number of pigs and stents, group assignment, and study progression.

examined. The other two pigs (mid-term group; one each from the single stent and pre-stent groups, total of seven stents) were allowed to grow for 2 another months (Table 1, Figure 1). We chose 2 months because previous studies show complete endothelialization of injured vessels in rabbits and pigs at 28 days [12-14].

Animal Experiments

Animal experiments were approved by the Institutional Animal Care and Use Committee at Purdue University. Yorkshire Cross piglets were used to allow rapid growth over a short period of time. Survival surgeries (i.e., catheterizations) were carried out at Purdue University facilities in collaboration with Cook Research Incorporated and Cook Medical. Pigs underwent a quarantine period and were examined by a veterinarian prior to catheterization procedures and weekly throughout the duration of the study.

Pigs were started on aspirin and clopidogrel 3 days prior to catheterization. Pigs were pre-medicated with tiletamine and zolazepam, and anesthesia was induced by a mixture of ketamine and xylazine. Pigs were intubated, and anesthesia was maintained with isoflurane (1.25–1.75% in 1.5–2.5 L/min oxygen) via a standard rebreathing anesthetic circuit for the remainder of the procedures. Intravascular access was obtained by carotid or femoral cut-down or percutaneous puncture using a modified Seldinger technique. Intramuscular antibiotic (ceftiofur crystalline) was given prior to stent implantation. After the procedure, anesthesia was discontinued, and pigs recovered on a raised floor pen. Pigs were medicated as necessary (meloxicam, butorphanol, or flunixin) to assure uncomplicated recovery and monitored every 15–30 min until they were alert and responsive. After catheterization, pigs were maintained on aspirin and clopidogrel throughout the growth phase to prevent stent thrombosis. Clinically, pigs were healthy and fully ambulatory throughout the study. Pig weight ranged from 9–11 kg at initial stent implantation to 98–119 kg at the time of euthanasia.

For euthanasia, pigs were anesthetized as above. Sodium nitroprusside was administered to reduce post-mortem vasospasm, and isoflurane level was increased to 5%. After approximately 5 min, pigs were euthanized by intravenous administration of potassium chloride. Death was verified by a lack of vital signs. After angiography and euthanasia, the abdominal cavity was opened and the aorta exposed. After gross examination of the aorta, the left ventricle and venous systems were cannulated. The aorta was perfusion-flushed with physiological saline until the effluent began to run clear. The stented area was then perfusion-fixed with Prefer fixative for approximately 10 min prior to immersion fixation in 10% neutral buffered formalin.

After the aorta was removed, pigs were submitted for full postmortem evaluation. Detailed macroscopic examination was performed by a board-certified vet-

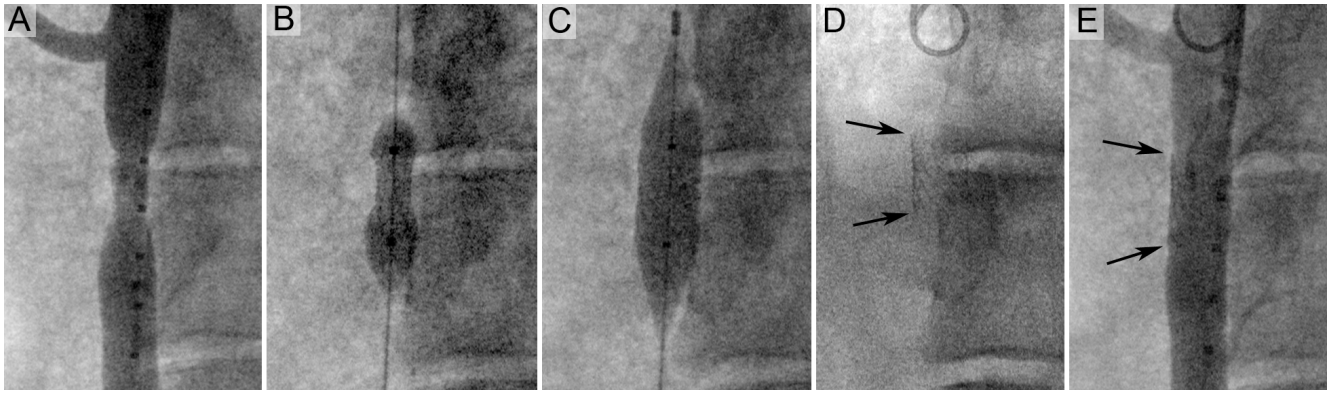

Figure 2. Pre-stenting technique. *Panel A*. Angiogram of the abdominal aorta with a 4-mm Cook Formula 418 stent implanted 5 months prior (stent diameter: 7.3 mm). *Panel B*. Implantation and anchoring of a Palmaz Genesis 1910 B stent mounted on a 10-mm Powerflex balloon. *Panel C*. Intentional fracture of the previously implanted Cook stent with simultaneous dilation of the newly implanted Palmaz Genesis stent using an ultra-high-pressure 12-mm Atlas balloon. *Panel D*. Radiograph showing the integrity and position of the newly implanted Palmaz Genesis stent inside the previously implanted Cook stent. *Panel E*. Angiogram showing vessel patency and minimal in-stent restenosis at the edges of the Palmaz Genesis stent 2 months after implantation (stent diameter: 9.9 mm). **Black arrows** indicate the edges of the Palmaz Genesis stent.

erinary pathologist, who assessed the stented blood vessel and adjacent areas for evidence of macroscopic tissue damage such as bleeding, contusion, rupture, and scarring. Major body systems including the brain, thoracic cavity viscera, peritoneal viscera, and hind limb muscles were examined grossly. Hind limb muscles were sectioned serially. In addition to stented regions of the aorta, a standard list of 33 tissues, as well as any grossly visible or suspected lesions, were collected for histopathology. Five muscle groups from each hind limb, lymph nodes regional to the hind limbs and descending aorta, and multiple sections of brain, lung, each kidney, liver, heart, spleen, and spinal cord were microscopically examined for any embolic lesion or stent fragment displacement.

Intentional Stent Fracture and Pre-Stenting Techniques

Serial dilation of small-diameter pre-mounted stents with intentional stent fracture and pre-stenting was feasible in a growing piglet model that mimics physiologic changes occurring in the vasculature of growing children. Small-diameter pre-mounted stents were successfully implanted in small vessels (Figure 2A). As expected, the patency of the growing blood vessel at the level of the stent was reduced by the previously implanted stents (Figure 2A); however, the vessel above and below the stent grew to almost double the original size of the vessel that held the original stent. Low-pressure balloons did not fully dilate and fracture the stents (Figure 2B), but ultra-high-pressure balloons achieved intentional stent fracture and re-dilation of previously implanted stents (Figure 2C). Stent dilation was performed in increments, and fracture occurred at the previously noted fracture diameter determined by bench testing [4]. In the single stent group, the stents were thinner and more difficult to visualize in the older pigs, so more atmospheres were used to ensure their breakage.

Radiographic, Angiographic, Gross Inspection, X-ray, Computed Tomographic, and Histopathologic Evaluation

Radiographic images and angiograms were obtained during all catheterization procedures. After euthanasia, necropsy was performed for gross inspection, histologic, and radiographic evaluation. The stented vessels were flushed with physiological saline for approximately 10 min followed by perfusion of Prefer fixative for 15 min prior to excision. Vessel diameter was measured using angiograms, and vessel luminal area was assessed using histologic samples.

Radiography. High-resolution radiography and micro computed tomography (CT) were performed on all stents after explant. High-resolution radiography was performed using a Kubtec Xpert 80-L w/

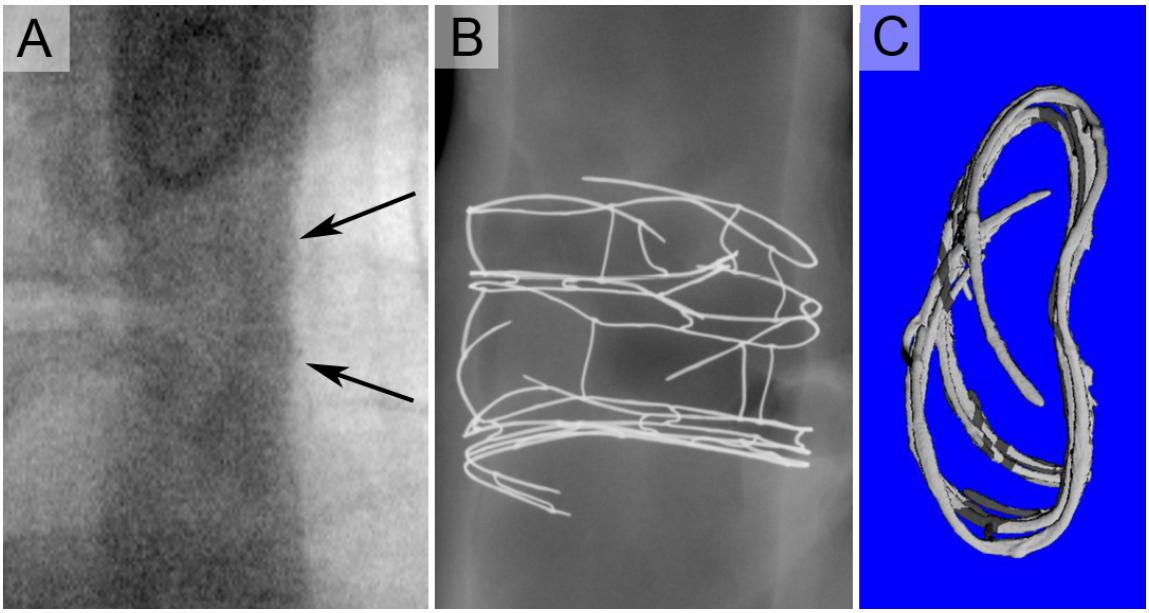

Figure 3. Reduced vessel patency and stent integrity after intentional fracture without pre-stenting. *Panel A*. Angiogram showing a small decrease in the diameter of the stented vessel segment compared with the adjacent area 2 months after intentional fracture and re-dilation of a 6-mm Cook Formula 418 stent with an ultra-high-pressure 16-mm Atlas balloon. **Black arrows** indicate the edges of the Cook stent. *Panel B*. High-resolution radiograph of the same segment showing fractured circumferential struts. *Panel C*. Down-the-barrel view of a three-dimensional rendition CT image of the same stent showing severely compromised luminal diameter in the antero-posterior dimension with struts protruding into the vessel lumen.

DIGI-VIEW 400, and micro CT was performed using a Scanco VivaCT40 System.

Histopathology. Perfusion-fixed, excised arteries were further immersion-fixed in 10% neutral buffered formalin. After dehydration though a serial gradient of alcohols and clearing in xylene, tissues were infiltrated with methyl methacrylate and polymerized in a water bath. Plastic embedded arteries, with stents in place, were cut on a diamond-encrusted saw blade into 30–50 µm sections. Proximal distal sections of stented artery (taken at 25% and 75% of the stent length) were stained with hematoxylin and eosin using routine techniques. Proximal and distal reference sections were trimmed from the fixed arteries, processed using routine paraffin histology techniques, and stained with hematoxylin and eosin. Morphometric measurements of each cross-section included vessel lumen area. Histopathological evaluation of stented vessels was performed by a board-certified veterinary pathologist. Cross-sections within each stent were evaluated for injury using an established semi-quantitative scoring system based on industry-standard consensus recommendations [15]. At each strut within a cross-section, vessel wall injury was scored as follows: 0 for no change in internal elastic lamina, 1 for rupture of internal elastic lamina, 2 for injury to tunica media, or 3 for injury to external elastic lamina and extending into or through the tunica adventitia. Each vessel had two cross-sections. The score for each cross-section was the sum of all injury scores for that cross-section divided by the number of total struts in the cross-section. The injury score for each group is the injury score for all cross-sections for the group divided by the total number of cross-sections for the group. Endothelialization was determined by the histological presence of endothelium over each strut within a cross-section. The degree of endothelialization is the percentage of endothelialized struts in the vessel.

Statistical Analysis

Descriptive statistical analysis was used to compare variables between pre-stent and single stent groups; data are expressed as median and interquartile range. Mann-Whitney tests were used to compare vessel lumen area, balloon size, degree of endothelialization,

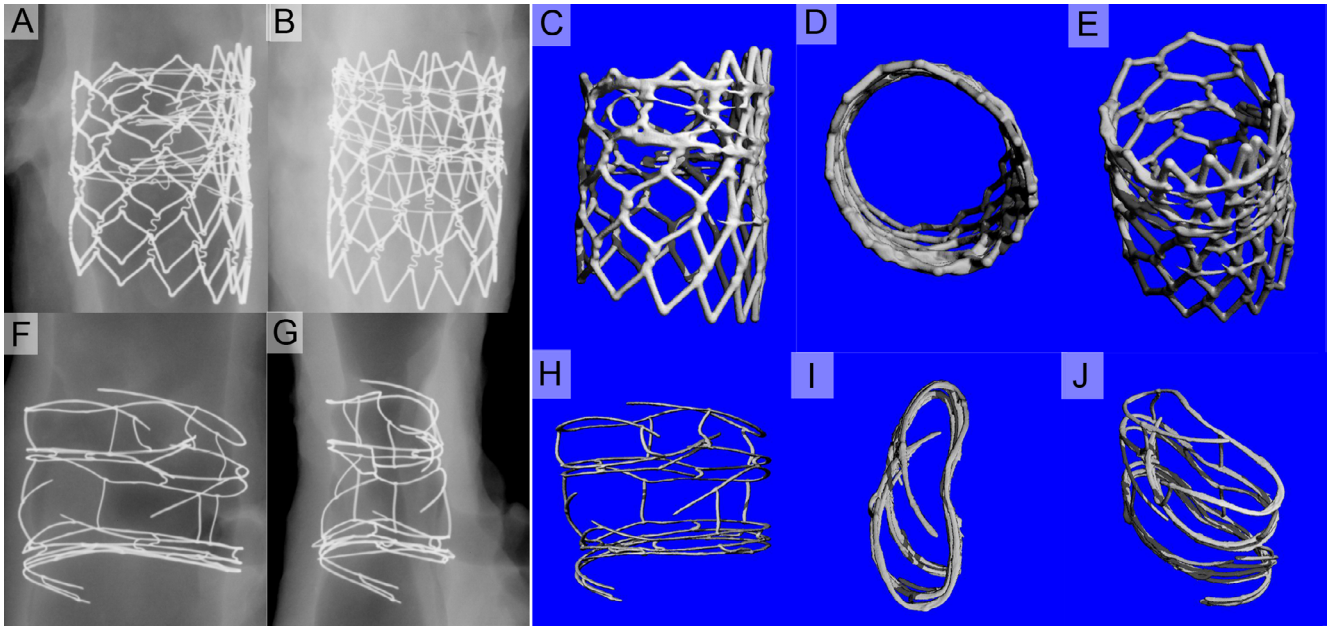

Figure 4. High-resolution radiographic and three-dimensional rendition CT images comparing pre-stenting at the time of stent fracture and single stent fracture. Intact stent integrity in the pre-stented segment maintained vessel patency, whereas loss of stent integrity after single stent fracture caused in-folding and compromised vessel lumen patency. *Panels A, B, C, D, and E*. Palmaz Genesis 1910 B stent implanted inside a Cook Formula 418 stent with simultaneous intentional fracture of the Cook stent. Images were taken 2 months after intentional fracture of the Cook stent. Images show intact internal stent integrity of the pre-stented vessel segment 2 months after implantation of the Palmaz Genesis stent with simultaneous intentional fracture of the 5-month previously implanted Cook stent. *Panels F, G, H, I, and J*. Cook Formula 418 stent 2 months after stent fracture (i.e., unzipping) without pre-stenting. Images show compromised stent integrity and vessel patency of the stented segment 2 months after intentional stent fracture and re-dilation of the 5-month previously implanted Cook stent.

Table 2. Comparison of outcome measures between the re-stent and single stent groups.

	Re-stent group	Single stent group	*p*-value
Lumen area (mm^2)* of stented blood vessels	108.9 (88.7-140.7) (n=4)	56.8 (47.3-72.8) (n=4)	**0.0190**
Vessel diameter loss (%)* 2 months after dilation	44 (26-59) (n=4)	75 (61-85) (n=4)	**0.0065**
Endothelialization (%) of stent struts	100 (89-100) (n=8)	73 (56-96) (n=8)	**0.0221**
Vessel wall injury score per struts	0.3 (0.26-0.45) (n=8)	0.5 (0.35-0.63) (n=8)	0.0673

Values expressed as median and interquartile range.
* Only the stents dilated with 16 mm balloon for diameter conformity

and vessel wall injury scores between groups; data are expressed as median and interquartile range. Mann-Whitney and Wilcoxon rank tests were used to compare the loss of luminal diameter from implantation to mid-term between groups; data are expressed as median change (%) and interquartile range. Vessel wall injury scores were compared between groups using unpaired t-tests and Mann-Whitney post-hoc tests for nonparametric data. Analyses were performed using Excel (Microsoft, Redmond, WA), GraphPad Prism (GraphPad, La Jolla, CA), and Instat 3 (Graph Pad, San Diego, CA) software. *P*-values < 0.05 were considered statistically significant.

Results

Vessel Patency and Luminal Diameter after Intentional Stent Fracture

After intentional stent fracture, we found significant vessel diameter loss in the single stent group

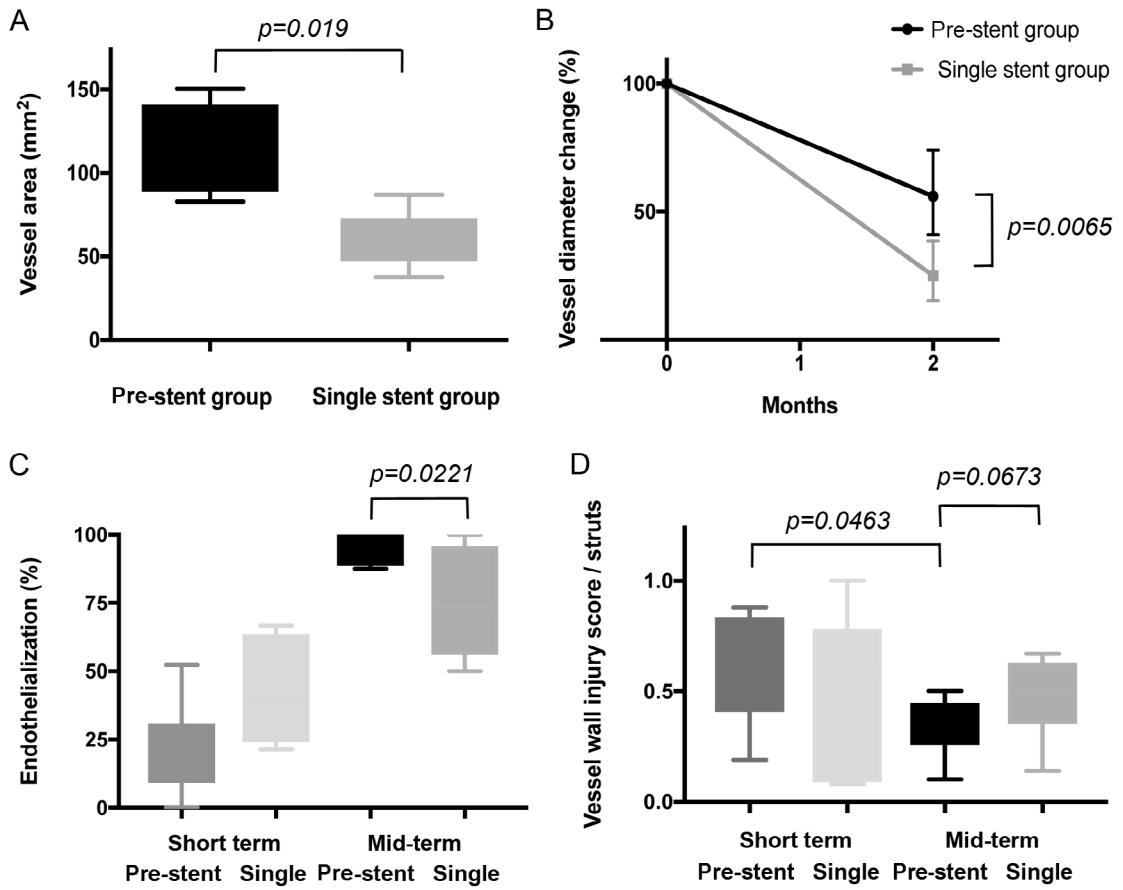

Figure 5. Comparison of vessel lumen diameter change, endothelialization, and vessel wall injury after intentional stent fracture between pre-stent and single stent groups. *Panel A*. Histomorphometric comparison of stented vessel lumen area 2 months after intentional stent fracture. The area of the stented vessel segments was significantly larger in the pre-stent group than in the single stent group. *Panel B*. The pre-stent group maintained larger angiographic lumen diameter, whereas the single stent group exhibited significant diameter loss due to stent in-folding and collapse 2 months after balloon angioplasty. *Panel C*. Pre-stenting allowed almost complete endothelialization 2 months after stent implantation, whereas endothelial coverage was significantly less in the single stent group due to luminal stent strut protrusion. *Panel D*. Comparison of vessel injury between pre-stent and single stent groups at short-term and mid-term evaluation. Vessel wall injury was similar at the time of stent fracture regardless of pre-stenting or unzipping without pre-stenting; however, injury score significantly improved 2 months after stent fracture in the pre-stent group but not in the single stent group. Data are shown as median, interquartile range, and range.

compared with the pre-stent group (Table 2). The degree of vessel diameter loss was subtle on traditional angiography (Figure 3A), but high-resolution radiography and rotational CT showed compromised vessel patency (Figure 3B and 33C) and revealed the mechanisms of vessel diameter loss in the single stent group as including stent in-folding, buckling, and collapse. This stent in-folding, buckling, and collapse was not present in the pre-stent group (Figure 4).

Consistent with the maintained vessel diameter as shown by angiography, radiography, and CT, the luminal area of the stented vessel segments measured by histomorphometry was significantly larger in the pre-stent group (109 mm^2 (89–141)) than in the single stent group (57 mm^2 (47–73), $P = 0.019$; Figure 5A). The angiographic vessel diameter of stented vessel segments was similar to that of adjacent naïve vessel segments in the pre-stent group, whereas the single stent group demonstrated significantly larger luminal diameter loss. Two months after angioplasty, compared with the balloon diameter used for dilation (we only compared segments after dilation with 16

mm for consistency of measurements), the pre-stent group showed only 44% (26–59) angiographic luminal diameter loss, whereas the single stent group showed 75% (62–85) luminal diameter loss ($P = 0.007$; Figure 5B).

Endothelialization and Exposed Stent Struts

There were no stent struts protruding into the lumen of vessels in the pre-stent group (Figure 4 and 6), whereas numerous naked (i.e., non-endothelialized) stent struts were noted in the lumen of vessels in the single stent group (Figures 6G, 6H, and 6I). Accordingly, the degree of endothelialization was markedly higher in the pre-stent group (100% (89–100)) than in the single stent group (73% (56–96), $P = 0.022$; Table 2, Figure 5C).

Vessel Wall Injury

Similar degrees of vessel wall injury were noted in the pre-stent group and single stent group at the time of intentional fracture (i.e., short-term) with scores of 0.51 and 0.59, respectively. However, at mid-term evaluation, the injury score in the pre-stent group was significantly improved (decrease from 0.51 to 0.31, $P = 0.046$), whereas the injury score in the single stent group was unchanged (0.5, $P > 0.05$; Figure 5D), although the difference between groups did not reach statistical significance ($P = 0.067$; Table 2, Figure 5D).

Lack of Injury to Adjacent Soft Tissue

Macroscopic examination of stented areas revealed a lack of external stent strut protrusion or transmural vessel injury in both the pre-stent and single stent groups (Figure 6). In both groups, the broken stent struts remained embedded in the vessel wall or exhibited inward protrusion due to the in-folding collapse of fractured stents (Figure 3, 4, and 6). There was no damage to the external part of the blood vessels or surrounding soft tissue (Figure 6C).

Microscopic examination of five muscle groups in the hind limb, lymph nodes regional to the hind limbs and descending aorta, and multiple sections of brain, lung, each kidney, liver, heart, spleen, and spinal cord showed no important lesions and no evidence of thromboembolism or stent fragment displacement in any downstream (i.e., hind limb muscles/regional lymph nodes) or systemic tissues.

Discussion

Our study demonstrates the feasibility of intentional stent fracture of previously implanted stents with simultaneous pre-stenting in an *in vivo* piglet model. Additionally, pre-stenting appears to provide appropriate vessel patency, prevents vessel diameter loss, improves endothelialization rate, and prevents intraluminal protrusion of stent struts. Moreover, pre-stenting appears to be safe, with no damage to surrounding soft tissue and no significant vessel wall injury.

Stented vessel diameter and cross-sectional area were significantly improved by pre-stenting during simultaneous intentional stent fracture of previously placed stents compared with no pre-stenting. Intentional stent fracture causes a loss of stent integrity with a dramatic decline in radial stiffness and strength [4]. This decrease in radial stiffness and strength allows the blood vessel to recoil more than with an intact stent. Moreover, an irregular stent fracture pattern may result in an irregular vessel wall shape. Both recoil and irregular shapes of blood vessels lead to compromised vessel lumen with decreased vessel diameter and cross-sectional area, consistent with our findings. As stent implantation is aimed at recovering areas of stenoses, it is of utmost importance that the stented vessel maintains appropriate patency. Simple stent fracture (i.e., unzipping) without the additional benefit of pre-stenting may not stabilize the vessel wall and may decrease vessel patency, thereby leading to restenosis and a significant pressure gradient.

Endothelial coverage allows appropriate blood vessel function and prevents thrombus formation at the vessel wall [16]. Fractured and not pre-stented fragments may protrude into the vessel lumen and prolong or even prevent complete endothelialization. Pre-stenting at the time of intentional fracture may prevent stent strut protrusion and thereby improve the chance of complete endothelialization with more rapid re-institution of physiologic vascular endothelial function.

Our observed vessel wall injury during pre-stenting was comparable to that after balloon angioplasty or single stent placement [6]. Incidental fracture of stents may cause severe vessel wall injury [17], and even intentional stent fracture *in vivo* (i.e., unzipping) may cause vessel wall damage due to an irregular

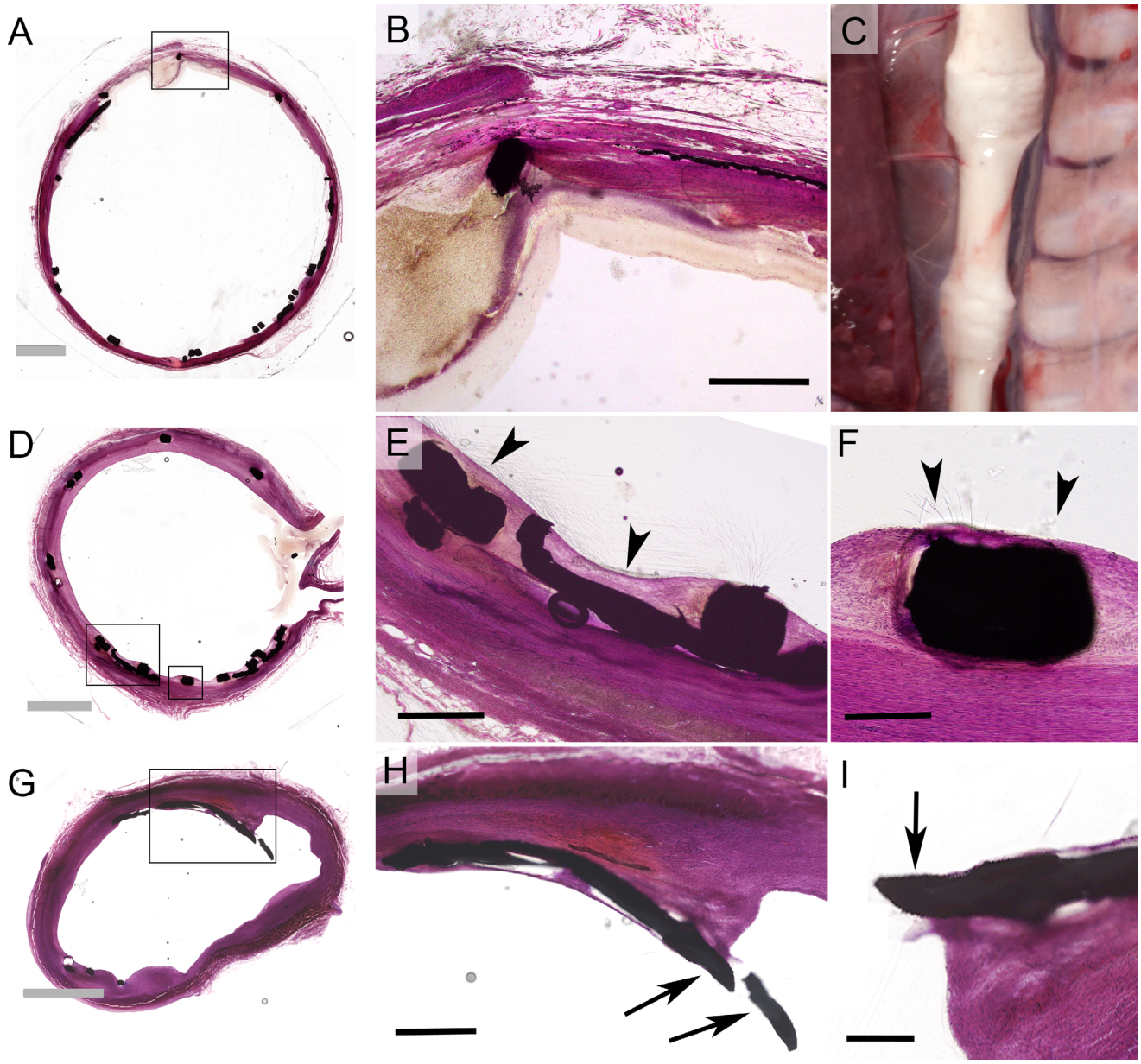

Figure 6. Vessel wall injury and endothelialization of blood vessels after pre-stenting compared with single stent implantation. Panels A, B, and C. Intentional stent fracture with pre-stenting caused only minimal vessel wall injury and did not result in transmural vessel injury or damage of surrounding soft tissue. *Panel A*. Localized dissection of the tunica media in a stented vessel immediately after stent implantation and lack of external protrusion of stent struts. *Panel B*. High-magnification image showing the extent of dissection and intramural hemorrhage immediately after stent placement. *Panel C*. Macroscopic picture showing no damage to the external surface of blood vessels despite the size discrepancy of stented segments. *Panels D, E, and F*. Pre-stenting allowed appropriate endothelialization and minimal vessel wall injury 2 months after stent placement. *Panel D*. Mid-term (i.e., 2 month) follow-up showed mild intimal and medial thickening in response to stent placement, no intraluminal protrusion of stent struts, and no dissection or pathologic vessel dilation. *Panels E and F*. High-magnification images showing almost complete endothelial coverage over stent struts 2 months after implantation. *Panel G*. Single stent implantation with intentional stent fracture (i.e., unzipping without pre-stenting) led to incomplete endothelialization due to intraluminal stent strut protrusion and decreased vessel lumen cross-sectional area. *Panels H and I*. High-magnification images showing stent strut protrusion without endothelial coverage. **Grey bars** in A, D, and G = 3 mm; **black bars** in B, E, and H = 0.5 mm and in F and I = 0.2 mm. **Black arrowheads** indicate endothelial coverage over stent struts, and **black arrows** point to bare metal struts protruding into the vessel lumen.

fracture pattern [11]. In our experience, pre-stenting at the time of intentional stent fracture caused no further injury to the vessel wall, and injury scores improved at mid-term evaluation.

Macroscopic examination of stented vessels provided no evidence of damage to the surrounding tissue or transmural vessel injury. This is important because *in vitro* testing of stents with intentional fracture produces an irregular fracture pattern, with many stent struts protruding tangentially [13]. These externally protruding stent fragments can penetrate through blood vessels and damage adjacent soft tissue, including arteriovenous malformations [11, 18, 19]. However, pre-stenting allows realignment of the struts of intentionally broken stents, which remain embedded in the vessel wall, in a more ideal circular fashion.

Our study has some limitations. The experiments were performed in a growing piglet model that has different growth velocity characteristics than humans. Nevertheless, this model has been employed in similar studies to mimic the growth of infants and small children [6]. Although the number of stents and animals were small, they were adequate to achieve statistical significance in the areas demonstrated. We assessed only one type of stent in this *in vivo* study, which was selected based on its superior characteristics in our *in vitro* bench testing [4]. Pressure gradients across the stents were not measured in all animals because we found only very small (2–5 mm Hg) gradients across stented segments in the few we measured. Moreover, our model was not intended to create significant coarctation with pressure gradients; rather, it was designed to evaluate the feasibility and characteristics of the pre-stenting technique.

In conclusion, our study shows that pre-stenting at the time of intentional pre-existing stent fracture provides advantages over simple stent fracture. Pre-stented vessels had larger vessel diameters, maintained better vessel patency, had more complete endothelialization, and showed no protrusion of stent struts into vessel lumens. These findings should be considered in small children requiring vessel angioplasty or stenting.

Acknowledgements

We deeply appreciate and thank the Foroni Family of Madrid, Spain for their generous contributions supporting this work and related stent studies. We thank William Schoenlein, Melissa Bible, Tracy Moller, Gena Brock, and Richard Sieber for their contributions and assistance with animal experiments. We also thank Omar El-Sabrout for his input in the study and review of the manuscript.

Conflict of Interest

The authors have no conflict of interest relevant to this publication.

References

1. Mullins CE, O'Laughlin MP, Vick GW 3rd, Mayer DC, Myers TJ, Kearney DL, et al. Implantation of balloon-expandable intravascular grafts by catheterization in pulmonary arteries and systemic veins. Circulation. 1988;77:188-199. PMID: 3335067
2. Rosenthal E, Qureshi SA. Stent implantation in congenital heart disease. Br Heart J. 1992;67:211-212. PMID: 1554537
3. O'Laughlin MP, Slack MC, Grifka RG, Perry SB, Lock JE, Mullins CE. Implantation and intermediate-term follow-up of stents in congenital heart disease. Circulation. 1993;88:605-614. PMID: 8339424
4. Bratincsak A, Moore JW, Gulker B, Choules B, Koren L, El-Said HG. Breaking the limit: Mechanical characterization of overexpanded balloon expandable stents used in congenital heart disease. Congenit Heart Dis. 2015;10:51-63. DOI: 10.1111/chd.12175
5. Sathanandam SK, Haddad LM, Subramanian S, Wright D, Philip R, Waller BR. Unzipping of small diameter stents: An in vitro study. Catheter Cardiovasc Interv. 2015;85:249-258. DOI: 10.1002/ccd.25596
6. Sathanandam SK, Kumar TK, Hoskoppal D, Haddad LM, Subramanian S, Sullivan RD, et al. Feasibility and safety of unzipping small diameter stents in the blood vessels of piglets. JACC Cardiovasc Interv. 2016;9:1138-1149. DOI: 10.1016/j.jcin.2016.02.035
7. Patel M, Justino H. Intentional stent fractures in structural heart disease: When breaking the chains is the only way! Catheter Cardiovasc Interv. 2013;81:179. DOI: 10.1002/ccd.24762
8. McElhinney DB, Bergersen L, Marshall AC. In situ fracture of stents implanted for relief of pulmonary arterial stenosis in patients with congenitally malformed hearts. Cardiol Young. 2008;18:405-414. DOI: 10.1017/S1047951108002424
9. Breinholt JP, Nugent AW, Law MA, Justino H, Mullins CE, Ing FF. Stent fractures in congenital heart disease. Catheter Cardiovasc Interv. 2008;72:977-982. DOI: 10.1002/ccd.21742

10. Kan J, Ge Z, Zhang JJ, Liu ZZ, Tian NL, Ye F, et al. Incidence and clinical outcomes of stent fractures on the basis of 6,555 patients and 16,482 drug-eluting stents from 4 centers. JACC Cardiovasc Interv. 2016;9:1115-1123. DOI: 10.1016/j.jcin.2016.02.025
11. Morray BH, McElhinney DB, Marshall AC, Porras D. Intentional fracture of maximally dilated balloon-expandable pulmonary artery stents using ultra-high-pressure balloon angioplasty: A preliminary analysis. Circ Cardiovasc Interv. 2016;9:e003281. DOI: 10.1161/CIRCINTERVENTIONS.115.003281
12. Van Belle E, Tio FO, Couffinhal T, Maillard L, Passeri J, Isner JM. Stent endothelialization. Time course, impact of local catheter delivery, feasibility of recombinant protein administration, and response to cytokine expedition. Circulation. 1997;95:438-448. PMID: 9008462
13. Taylor AJ, Gorman PD, Kenwood B, Hudak C, Tashko G, Virmani R. A comparison of four stent designs on arterial injury, cellular proliferation, neointima formation, and arterial dimensions in an experimental porcine model. Catheter Cardiovasc Interv. 2001;53:420-425. DOI: 10.1002/ccd.1194
14. Schwartz RS, Huber KC, Murphy JG, Edwards WD, Camrud AR, Vlietstra RE, et al. Restenosis and the proportional neointimal response to coronary artery injury: results in a porcine model. J Am Coll Cardiol. 1992;19:267-274. PMID: 1732351
15. Schwartz RS, Edelman E, Virmani R, Carter A, Granada JF, Kaluza GL, et al. Drug-eluting stents in preclinical studies: updated consensus recommendations for preclinical evaluation. Circ Cardiovasc Interv. 2008;1:143-153. DOI: 10.1161/CIRCINTERVENTIONS.108.789974
16. van Hinsbergh VW. Endothelium--role in regulation of coagulation and inflammation. Semin Immunopathol. 2012;34:93-106. DOI: 10.1007/s00281-011-0285-5
17. McElhinney DB, Marshall AC, Schievano S. Fracture of cardiovascular stents in patients with congenital heart disease: theoretical and empirical considerations. Circ Cardiovasc Interv. 2013;6:575-585. DOI: 10.1161/CIRCINTERVENTIONS.113.000148
18. Bernier PL, Hallbergson A, Schachtner SK, Rome JJ, Gaynor JW. Aortopulmonary fistula after outflow tract stent in repaired truncus. Ann Thorac Surg. 2014;98:e55-e57. DOI: 10.1016/j.athoracsur.2014.06.090
19. Page M, Nastase O, Maes F, Kefer J, Sluysmans T, Poncelet A, et al. Aortopulmonary fistula after multiple pulmonary artery stenting and dilatation for postarterial switch supravalvular stenosis. Case Rep Cardiol. 2015;2015:371925. DOI: 10.1155/2015/371925

Cite this article as: Bratincsák A, Van Alstine W, Koren L, Stoughton K, Negrón-Garcia J, Ragheb A, El-Sabrout H, Moore JW, el-Said H. Intentional Fracture of Previously Placed Stents: Impact of Pre-stenting in a Piglet Model. Structural Heart Disease. 2017;3(6):165-175. DOI: https://doi.org/10.12945/j.jshd.2017.030.17

JSHD
Journal of Structural Heart Disease

Case Report

Journal of Structural Heart Disease, December 2017, Volume 3, Issue 6:176-179
DOI: https://doi.org/10.12945/j.jshd.2017.025.17

Received: May 31, 2017
Accepted: June 29, 2017
Published online: December 2017

Elective Stent Implant in the Obstructed Vertical Vein of Supracardiac Total Anomalous Pulmonary Venous Connection Prior to Operative Repair

Elisa Rhee, MBBCh, BAO[1], John P. Breinholt, MD[1*]

[1] Department of Pediatrics, University of Texas Health Science Center at Houston, Houston, Texas, United States

Abstract

Background: Total anomalous pulmonary venous connection (TAPVC) comprises 2% of congenital heart disease cases. Obstructed TAPVC typically presents with respiratory distress secondary to pulmonary congestion. We report a case of an infant patient who was electively referred to catheterization for stent placement to relieve vertical vein (VV) stenosis. Our objective was to prevent the emergent need for surgical intervention while allowing additional growth before surgery.

Case Presentation: A 7-day-old, late pre-term, small for gestational age male infant was transferred from an outside institution. He was initially placed on nasal cannula due to oxygen saturation around 80% but progressed to continuous positive airway pressure and had a chest X-ray suggestive of pulmonary edema. Echocardiography revealed supracardiac TAPVC, a small apical muscular ventricular septal defect, and a moderate secundum atrial septal defect. On admission, the patient was clinically stable with a baseline oxygen saturation of 72% on 40% oxygen. Echocardiography confirmed supracardiac TAPVC and also showed an obstruction with a mean gradient of 22 mmHg in the VV. The desire to optimize the patient's clinical stability led to the decision to undergo cardiac catheterization for stent implantation in the VV. Immediately following the procedure, the patient's hemodynamics improved, with a pressure gradient between the pulmonary venous confluence and the left innominate vein of 4 mmHg.

Conclusions: Over the last decade, surgical outcomes of TAPVC repair have improved with better control of pulmonary hypertension and preoperative clinical stabilization due to more aggressive medical management. This case presents an opportunity to consider an elective interventional strategy that palliates the disease to prevent an urgent need for definitive repair.

Key Words

TAPVC • Interventional • Obstructed • Vertical vein • Elective

Introduction

Total anomalous pulmonary venous connection (TAPVC) is a rare cardiac defect that comprises 2% of congenital heart disease cases [1]. TAPVC encompasses different anatomic subtypes in which pulmonary veins fail to connect directly to the left atrium and drain to the right atrium via an anomalous venous connection [2, 3]. Supracardiac TAPVC is the most common type, comprising about 45% of cases [2]. A left-sided vertical vein (VV) accounts for 70% of the connections between the pulmonary confluence and the right atrium, and stenosis occurs in approximately 40% of cases [3].

Obstructed TAPVC typically presents with respiratory distress secondary to pulmonary congestion,

Fax +1 203 785 3346
E-Mail: jshd@scienceinternational.org
http://structuralheartdisease.org/

ISSN 2326-4004

Accessible online at:
http://structuralheartdisease.org/

* Corresponding Author:
John P. Breinholt, MD
Department of Pediatrics
University of Texas Health Science Center at Houston
6410 Fannin Street, Suite 425, , Houston, TX 77030, USA
Tel. +1 713 500 5738; E-Mail: john.p.breinholt@uth.tmc.edu

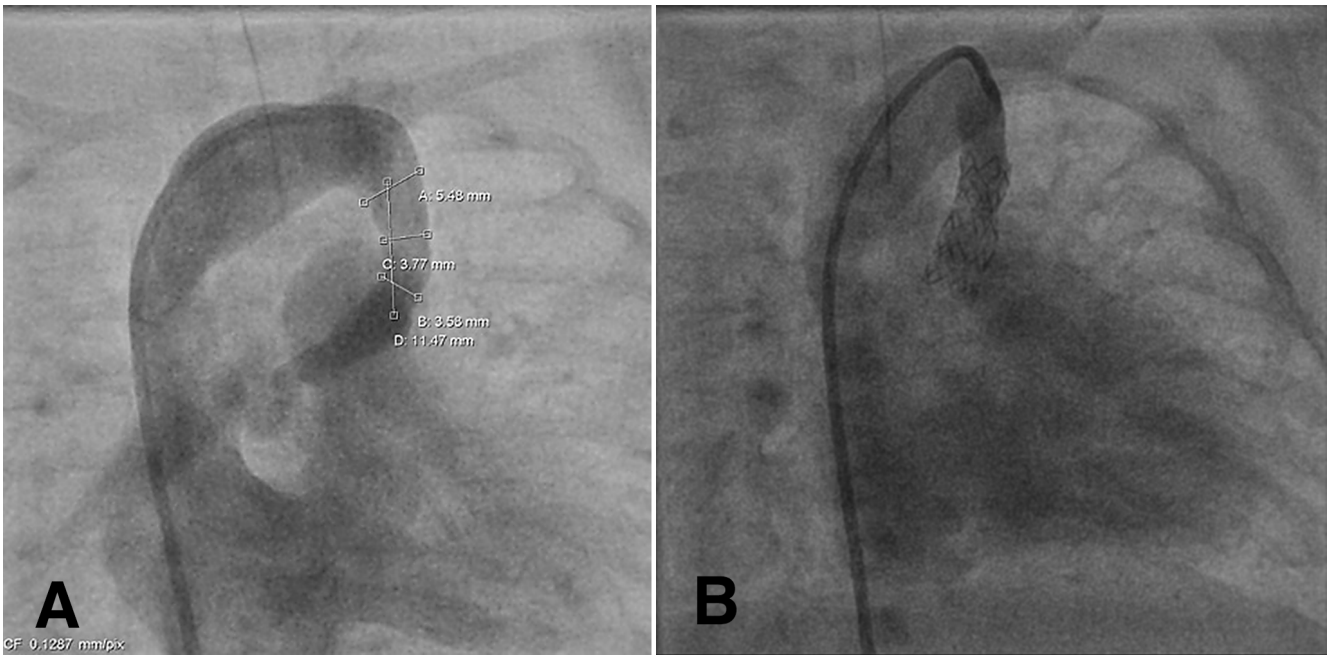

Figure 1. *Panel A.* Cardiac angiography prior to stent placement. The confluence narrowing is 3.6mm with the superior aspect of the vertical vein measuring 5.5mm. *Panel B.* Cardiac angiography after the two stents were implanted, with the second stent telescoped proximally within the initial stent.

cyanosis, and metabolic acidosis [4]. It is traditionally considered a surgical emergency. Emergent stenting of the VV is rarely reported but has been performed when a patient is considered a poor candidate for surgical repair [4-6]. Pulmonary venous obstruction is associated with poor prognosis and a high risk of operative mortality [7, 8].

Here, we report a case of an infant patient who was electively referred to catheterization for stent placement to relieve VV stenosis. Our objective was to prevent the emergent need for surgical intervention while allowing additional growth before surgery.

Case Presentation

A 7-day-old, former 36 6/7 week, 2.4 kg, small for gestational age male infant was transferred from an outside institution. At the time of delivery, he was noted to have poor respiratory effort and a heart rate below 100 beats per minute. Chest compressions were provided for less than 1 min, and his APGAR scores were 5 and 7 at 1 and 5 min, respectively. The patient was noted to have oxygen saturation of roughly 80%, requiring blow by oxygen. He was initially placed on nasal cannula, but over the next 7 days progressed to continuous positive airway pressure and had a chest X-ray suggestive of pulmonary edema. An echocardiogram at that time revealed supracardiac TAPVC, a small apical muscular ventricular septal defect with right-to-left shunt, and a moderate secundum atrial septal defect with right-to-left shunt.

On admission, the patient was stable with a baseline oxygen saturation of 72% on 40% oxygen. An echocardiogram was performed that confirmed supracardiac TAPVC but demonstrated an obstruction in the VV with a mean gradient of 22 mmHg. All pulmonary veins drained to a confluence behind the left atrium and communicated to the innominate vein via a VV.

The patient's size and the desire to optimize his clinical stability led to the decision to undergo cardiac catheterization for stent implantation in the VV (Figure 1A). Femoral vein access was achieved, and a 4-F angled Glide catheter (Terumo, Somerset, NJ, USA) was advanced prograde into the VV. A 17 mmHg pressure gradient between the pulmonary venous confluence and the left innominate vein was recorded. A V-18 Control wire (Boston Scientific, Marlborough,

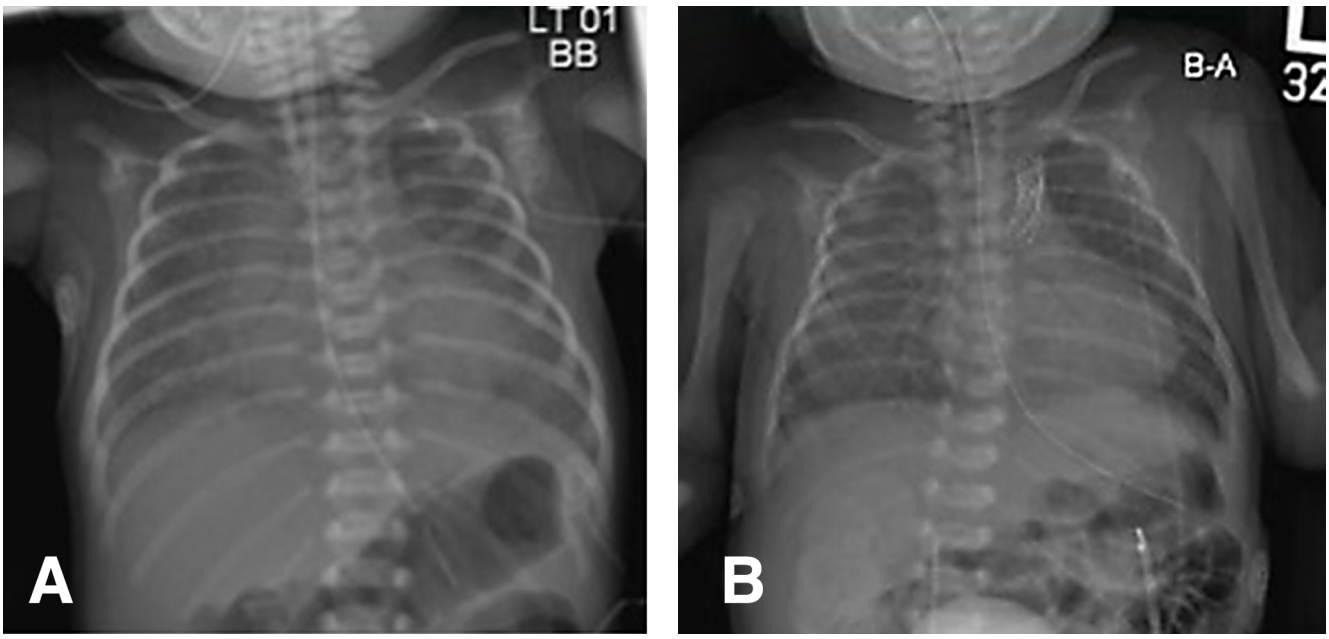

Figure 2. *Panel A.* Chest radiograph 1 day prior to stent placement. Diffuse pulmonary edema is seen. *Panel B.* Chest radiograph 1 day after stent placement in the vertical vein. The stents are visible along the left sternal border. There is improvement in the pulmonary edema.

MA, USA) was advanced into the right lower pulmonary vein, and the Glide catheter was exchanged for a Palmaz Blue 6 × 16 mm stent (Cordis, Fremont, CA, USA) that was deployed in the VV. Due to a persistent residual gradient, a Palmaz Blue 6 × 12 mm stent was telescoped proximally within the prior stent to ensure resolution of the obstruction within the VV (Figure 1B). Repeat hemodynamics demonstrated a pressure gradient between the pulmonary venous confluence and the left innominate vein of 4 mmHg. Oxygen saturation improved to 95% on 50% oxygen, which was reduced to room air over 48 hours. Repeat chest X-ray showed improvement of the pulmonary edema (Figure 2A and 2B).

Over the following 3 weeks, pulmonary edema developed again despite medical management with diuretics. At 26 days of age, the patient had gained approximately 200 g and underwent TAPVC repair. He recovered well, was extubated, and weaned to room air by postoperative day 5. He was discharged on postoperative day 21 on once daily furosemide.

Discussion

Low birth weight is an independent risk factor in the operative management of obstructive TAPVC [5, 6, 9]. Patients who undergo emergent VV stent implantation prior to definitive surgery often present with respiratory distress and cyanosis secondary to pulmonary congestion [4]. In this case, the patient showed no evidence of pulmonary venous obstructive disease, the presentation of which leads to emergent surgery. The patient's respiratory support was more suggestive of pulmonary overcirculation due to the large left-to-right shunt produced by the anomalous pulmonary venous return. Our clinical strategy was to allow the patient to achieve additional somatic growth to mitigate the increased morbidity and mortality observed in low birth weight neonates with this disease.

Over the last decade, surgical outcomes of TAPVC repair have improved with better control of pulmonary hypertension and preoperative clinical stabilization due to more aggressive medical management [6, 9]. Our case presents an opportunity to consider an interventional strategy that palliates the disease to prevent an urgent need for definitive repair. Stent

implantation in the VV provides a bridge that allows further somatic growth and improved pulmonary mechanics from obstruction relief.

Supracardiac TAPVC is a rare congenital cardiac defect in which obstruction of the VV approaches 40% [3]. Elective stent implant in the VV as a palliative procedure may allow additional somatic growth to reduce mortality and morbidity at the time of surgery. Therefore, urgent surgery is avoided, with time allowing for planning and resolution of symptoms prior to definitive repair.

Conflict of Interest

The authors have no conflict of interest relevant to this publication.

Comment on this Article or Ask a Question

References

1. Michielon G, Di Donato RM, Pasquini L, Giannico S, Brancaccio G, Mazzera E, et al. Total anomalous pulmonary venous connection: Long-term appraisal with evolving technical solutions. Eur J Cardiothorac Surg. 2002;22:184-191. PMID: 12142183
2. Hirsch JC, Bove EL. Total anomalous pulmonary venous connection. Multimed Man Cardiothoarcic Surg. 2007;507:mmcts.2006.002253. DOI: 10.1510/mmcts.2006.002253
3. Brown VE, Lange MD, Dyar DA, Impastato LW, Shirali GS. Echocardiographic spectrum of supracardiac total anomalous pulmonary venous connection. J Am Soc Echocardiogr. 1998;11:289-293. PMID: 9560753
4. Kobayashi D, Forbes TJ, Aggarwal S. Palliative stent placement in vertical vein in a 1.4 kg infant with obstructed supracardiac total anomalous pulmonary venous connection. Catheter Cardiovasc Interv. 2013;82:574-580. DOI: 10.1002/ccd.24632
5. Burkhardt EB, Stiller B, Grohmann J. Stenting of the obstructed ductus venosus as emergency and bridging strategy in a very low birth weight infant with infradiaphragmatic total anomalous pulmonary venous connection. Catheter Cardiovasc Interv. 2014;84:820-823. DOI: 10.1002/ccd.25560
6. Lo-A-Njoe SM, Blom NA, Bökenkamp R, Ottenkamp J. Stenting of the vertical vein in obstructed total anomalous pulmonary venous return as rescue procedure in a neonate. Catheter Cardiovasc Interv. 2006;67:668-670. DOI: 10.1002/ccd.20715
7. Hyde JA, Stümper O, Barth MJ, Wright JG, Silove ED, de Giovanni JV, et al. Total anomalous pulmonary venous connection: outcome of surgical correction and management of recurrent venous obstruction. Eur J Cariothorac Surg. 1999;15:735-740. PMID: 10431851
8. Hammon JW Jr, Bender HW Jr, Graham TP Jr, Boucek RJ Jr, Smith CW, Erath HG Jr. Total anomalous pulmonary venous connection in infancy. Ten years' experience including studies of postoperative ventricular function. J Thorac Cardiovasc Surg. 1980;80:544-551. PMID: 7421289
9. Padalino MA, Cavalli G, De Franceschi M, Mancuso D, Maschietto N, Vida V, et al. Surgical outcomes of total anomalous pulmonary venous connection repair: A 22-year experience. J Card Surg. 2014;29:678-685. DOI: 10.1111/jocs.12399

Cite this article as: Rhee E, Breinholt JP. Elective Stent Implant in the Obstructed Vertical Vein of Supracardiac Total Anomalous Pulmonary Venous Connection Prior to Operative Repair. Structural Heart Disease. 2017;3(6):176-179. DOI: https://doi.org/10.12945/j.jshd.2017.025.17

JSHD
Journal of Structural Heart Disease

Case Report

Journal of Structural Heart Disease, December 2017, Volume 3, Issue 6:180-186
DOI: https://doi.org/10.12945/j.jshd.2017.026.17

Received: June 06, 2017
Accepted: June 15, 2017
Published online: December 2017

Successful First-in-Man Concomitant Transapical Transcatheter Aortic and Mitral Valve Replacements for Severe Native Aortic and Mitral Valve Stenosis Using the Edwards Certitude Delivery System

Anwar Tandar, MD[1], Jason P. Glotzbach, MD[2], Frederick G.P. Welt, MD[1], Vikas Sharma, MD[2], Kelsee Browning, AGNP-C[1], Craig H. Selzman, MD[2], Abdulfattah Saidi, MD[1*], David A. Bull, MD[2]

[1] Division of Cardiovascular Medicine, University of Utah School of Medicine, Salt Lake City, Utah, United States

[2] Division of Cardiothoracic Surgery, University of Utah School of Medicine, Salt Lake City, Utah, United States

Abstract

Transcatheter aortic valve replacement (TAVR) has become the treatment of choice for high or intermediate risk patients with symptomatic severe aortic stenosis. Transcatheter mitral valve replacement (TMVR) for native mitral stenosis is still under investigation in clinical trials. Results from a global registry, however, show that TMVR in patients with severe mitral annulus calcification is feasible but associated with significant adverse events. Simultaneous TAVR and TMVR on native valves has only been reported twice. Here, we report the first case of simultaneous TAVR and TMVR for native aortic and mitral stenosis using the Edwards Certitude transapical delivery system.

Key Words

Native aortic stenosis • Native mitral stenosis • Simultaneous • Double valve • Transcatheter valve replacement • Transapical approach

Introduction

Transcatheter aortic valve replacement (TAVR) has emerged as the treatment of choice for patients with severe aortic stenosis who are deemed to be at high or intermediate risk for surgery [1, 2]. Transcatheter mitral valve replacement (TMVR) for inoperable severe calcific native mitral stenosis is currently under investigation in clinical trials [3]. Results from a global registry show that TMVR, when performed in highly selected patients, results in significant adverse events [4]. Simultaneous TAVR and TMVR of stenotic native valves has only been reported in two cases [5, 6]. Here, we report the first case of simultaneous TAVR and TMVR for severely stenotic native aortic and mitral valves in a high-risk patient using the Edwards Certitude transapical delivery system (Edwards Lifesciences, Irvine, CA, USA) (Figure 1).

Case Presentation

The patient was a 71-year-old man with symptomatic severe aortic stenosis (mean gradient, 53 mmHg; aortic valve area, 0.7 cm^2; maximum aortic valve velocity, 4.1 m/s; Figure 2 and Figure 3) and heavily calcified severe mitral stenosis (mean gradient, 12 mmHg; mitral valve area, 1 cm^2; Figure 4 and Figure

Fax +1 203 785 3346
E-Mail: jshd@scienceinternational.org
http://structuralheartdisease.org/

ISSN 2326-4004

Accessible online at:
http://structuralheartdisease.org/

* Corresponding Author:
Abdulfattah Saidi, MD
Division of Cardiovascular Medicine
University of Utah School of Medicine
50 North Medical Drive, Salt Lake City, UT 84132, USA
Tel. +1 801 647 2390; Fax: +1 801 585 3362; E-Mail: abdulfattah.saidi@hsc.utah.edu

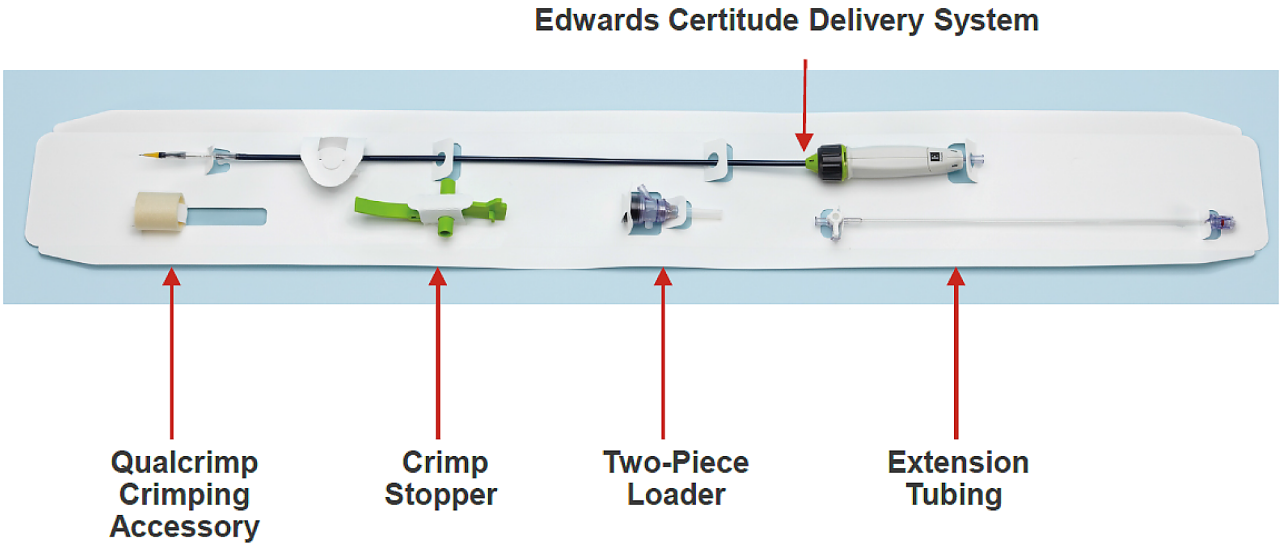

Figure 1. Edwards Certitude delivery system.

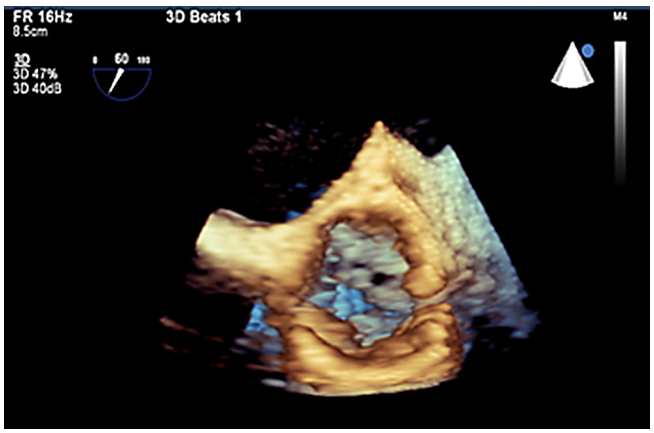

Figure 2. Three-dimensional TEE showing a heavily calcified aortic valve with severe stenosis.

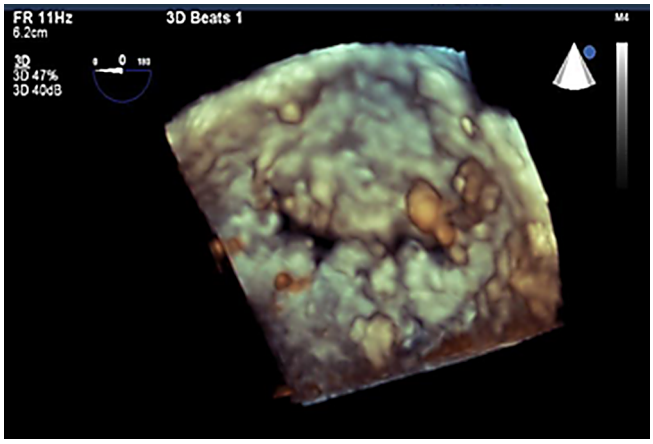

Figure 3. TEE short axis view showing a heavily calcified aortic valve.

5) with a Wilkins score of 12 and mean pulmonary artery pressure of 43 mmHg. His left ventricular ejection fraction was 44%, and he showed Class III New York Heart Association symptoms. His medical history also included coronary disease status post-coronary artery bypass graft, peripheral artery disease status post-femoral-femoral artery bypass, porcelain aorta, severe chronic obstructive pulmonary disease, type II diabetes mellitus, and sick sinus syndrome.

After evaluation by a multidisciplinary heart team, the patient was deemed to be a prohibitively high-risk candidate for surgical aortic valve replacement due to a Society of Thoracic Surgeons mortality risk score greater than 10% and the presence of a porcelain aorta on imaging studies. Balloon mitral valvuloplasty was contraindicated due to a high Wilkins score. Therefore, we made the decision to proceed with simultaneous TAVR and TMVR.

Valve analysis was performed using helical computed axial tomography (CT) scanning with 3mensio Structural Heart (3mensio Medical Imaging BV, Bilthoven, Netherlands) and OsiriX three-dimensional

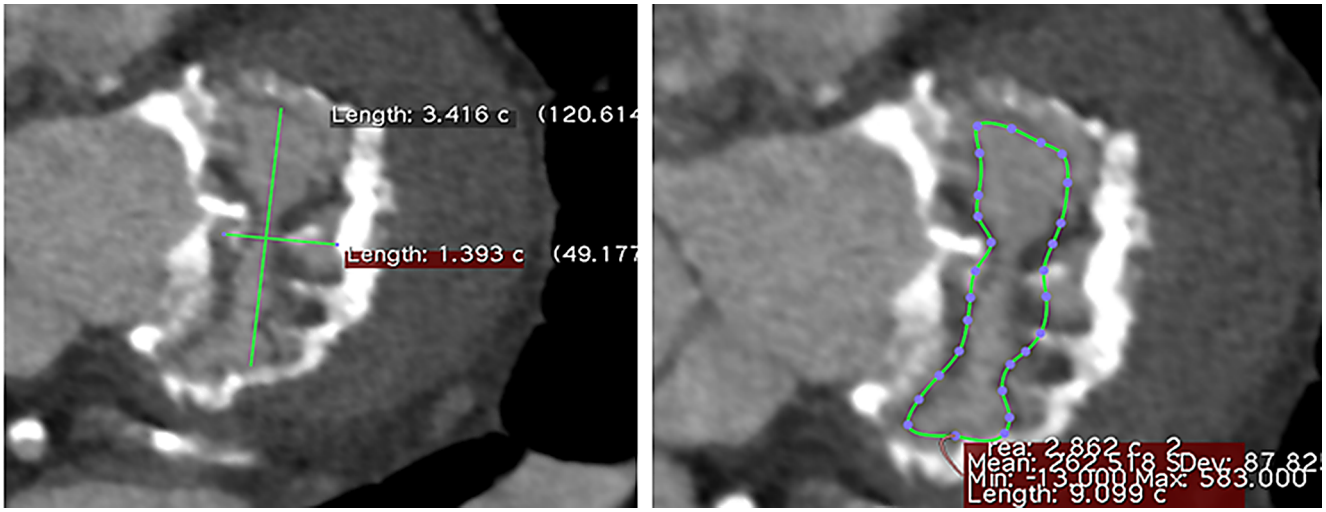

Figure 4. Three-dimensional TEE showing a heavily calcified mitral valve with severe stenosis..

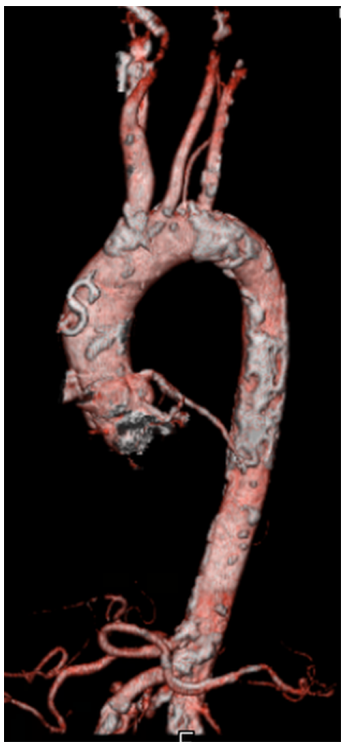

Figure 5. TEE four chamber view with color doppler showing severe mitral stenosis.

reconstruction software (Pixmeo SARL, Bernex, Switzerland). This analysis demonstrated an aortic annulus area of 480 mm^2, which was suitable for a 26-mm Edwards SAPIEN 3 (Edwards Lifesciences, Irvine, CA, USA) valve. The mitral valve area was 286 mm^2, which was suitable for a 29-mm Edwards SAPIEN 3 valve**.**

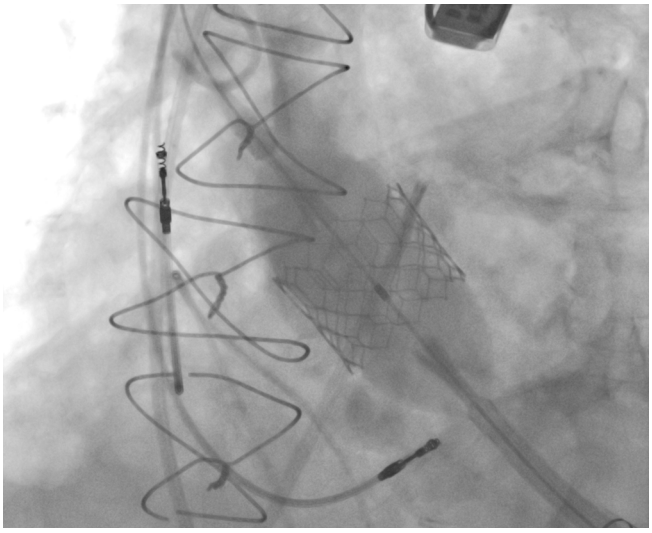

Figure 6. Fluoroscopy clip showing deployment of the SAPIEN 3 valve in the aortic position.

The CT scan also showed a porcelain aorta.

The procedure took place under general anesthesia in a hybrid operating room. A Certitude delivery system was inserted into the apex through a limited left anterior thoracotomy utilizing 2-0 plegeted braided polyester sutures as mattress pursestrings (Ethicon, Somerville, NJ, USA). A 0.035" guidewire was advanced into the ascending aorta and then exchanged with an Extra Stiff Amplatz wire. The 26-mm SAPIEN 3 valve was advanced and deployed during rapid pacing (Figure 6). Transesophageal echocardiography (TEE) showed that the prosthesis was in an

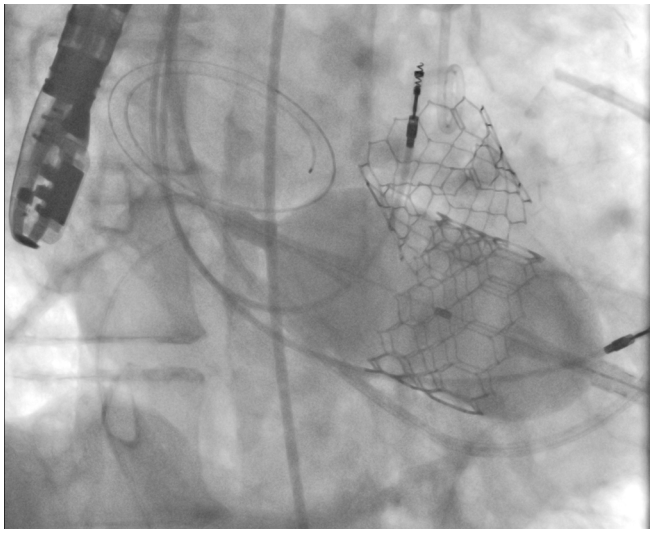

Figure 7. TEE biplane view of the aortic valve showing the SAPIEN 3 valve in the appropriate aortic position.

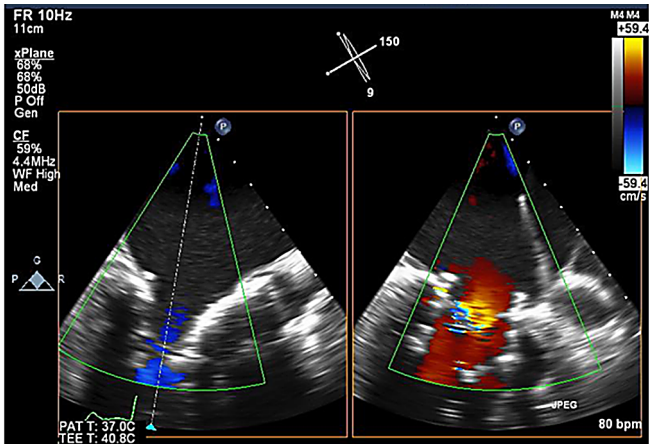

Figure 8. Fluoroscopy clip showing deployment of the inverted SAPIEN 3 valve in the mitral position.

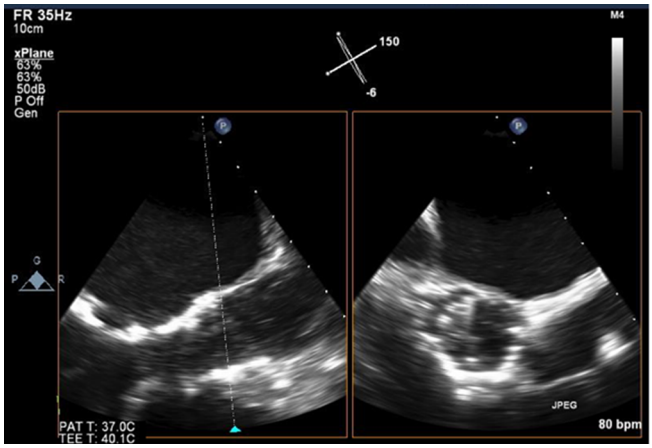

Figure 9. TEE showing the inverted SAPIEN 3 valve in the appropriate mitral position.

optimal position without paravalvular leak (Figure 7). The mean gradient across the prosthetic valve was 5.7 mmHg.

Subsequently, the TAVR delivery system was removed, and the Certitude sheath was kept in place. A 0.035" straight-tip wire was used to cross the mitral valve and then exchanged with an Inoue wire. To achieve maximum expansion, 4 mL was added to the 29-mm SAPIEN 3 balloon. A coplanar fluoroscopic view was obtained using the mitral annular calcification as a landmark. The valve was deployed during rapid pacing using fluoroscopic and live TEE guidance (Figure 8). TEE showed that the prosthesis was in an optimal position (Figure 9), with trivial paravalvular leak and a mean gradient of 3.5 mmHg. The left ventricle outflow tract gradient was 12 mmHg. Postdilation with an additional 2 mL (total of 6 mL) was performed to flair the atrial side of the Sapien valve and minimize the risk of valve migration. Prior to discharge (i.e., 5 days after the procedure), transthoracic echocardiography showed normal function of both prostheses without paravalvular leaks. At 2-month follow-up, the patient continued to do well. Follow-up transthoracic echocardiography showed no changes compared with prior study.

Discussion

TAVR has been found to be non-inferior to surgical aortic valve replacement in patients with severe atrial stenosis deemed to be at high or intermediate surgical risk [1, 2]. These patients often have concomitant mitral stenosis with a high Wilkins score, barring them from mitral balloon valvuloplasty. The option of performing TMVR of native mitral stenosis at the same time as TAVR, although not previously studied, has been reported in two cases [5, 6]. To the best of our knowledge, this is the first simultaneous TAVR and TMVR of native aortic and mitral valves stenoses utilizing a single transapical access with the Edwards Certitude delivery system.

Because is a complex and novel approach, selecting the appropriate candidate is key for success of this procedure. It is of utmost importance to obtain accurate measurements of both aortic and mitral annuli and to select the appropriate prosthesis size and minimize the risk of interference given the anatomi-

cal proximity of the two valves.

Edwards SAPIEN S3 was chosen as it is the only transcatheter valve available that can be reverse-mounted to accommodate the transapical approach. Additionally, the SAPIEN 3 valve provides the option of balloon hyperexpansion if needed to minimize the risk of migration and paravalvular leak, especially in the mitral position. The sequence of valve implantation is controversial. Salaun et al. [7] speculated that starting with mitral valve implantation may result in obstruction of the aortic prosthesis. Bauernschmitt et al. [5] chose to implant the mitral valve first due to the anatomical proximity and concern for compression of the smaller aortic valve while implanting the larger mitral prosthesis. In Elkharbotly's case [6], the aortic valve was placed first. In our case, the aortic valve was implanted first due to the critical nature of the aortic stenosis and in case of unexpected complications occurring during mitral valve intervention.

It is difficult to estimate the risk of mitral prosthesis migration. In the Bauernschmitt case [5], valve migration was not noted before the patient died from malignancy 9 months after implantation. In the Elkharbotly case [6], the reported 6-month follow-up was free of valve migration. Bapat et al. [8], in a valve-in-valve case, reported the migration of a SAPIEN prosthesis from the mitral position. In our case, we decided to hyperexpand the balloon in the mitral position to maximize valve fixation and minimize the risk of migration. Hyperexpanding the mitral prosthesis may theoretically cause compression of the aortic valve or left ventricular outflow tract obstruction. Fortunately, the postdeployment left ventricular outflow tract gradient was only 12 mmHg.

In conclusion, simultaneous TAVR and TMVR for native aortic and mitral valve stenosis may be safe in highly selected inoperable patients. The long-term safety and outcome of simultaneous TAVR and TMVR are not known, and more investigation is needed to validate this approach.

Conflict of Interest

The authors have no conflict of interest relevant to this publication.

Comment on this Article or Ask a Question

References

1. Leon MB, Smith CR, Mack MJ, Miller CD, Moses JW, Lars S, et al. Transcatheter aortic-valve implantation for aortic stenosis in patients who cannot undergo surgery. N Eng J Med. 2010;363:1597-1507. DOI: 10.1056/NEJMoa1008232
2. Reardon MJ, Van Mieghem NM, Popma JJ, Kleiman NS, Sondergaard L, Mumtaz M, et al. Surgical or transcatheter aortic-valve replacement in intermediate-risk patients. N Eng J Med. 2017;376:1321-1331. DOI: 10.1056/NEJMoa1700456
3. Guerrero ME. Mitral Implantation of TRAnscatheter vaLves (MITRAL). ClinicalTrails.gov: NCT02370511
4. Gurrero M, Dvir D, Himbert D, Urene M, Eleid M, Greenbaum A, et al. Transcatheter mitral valve replacement in native mitral valve disease with severe mitral annular calcification: Results from the first multicenter global registry. JACC Cardiovascular Interv. 2016;9:1361-1371. DOI: 10.1016/j.jcin.2016.04.022
5. Bauernschmitt R, Bauer S, Liewald C, Emini R, Oechsner W, Beer M, et al. First successful transcatheter double valve replacement from a transapical access and nine-month follow up. EuroIntervention. 2017;17:1645-1648. DOI: 10.4244/EIJ-D-16-00896
6. Elkharbotly A, Delago A, El-Hajjar M. Simultaneous transapical transcatheter aortic valve replacement and transcatheter mitral valve replacement for native valvular stenosis. Catheter Cardiovasc Interv. 2016;87:1347-1351. DOI: 10.1002/ccd.26078
7. Salaun E, Pankert M, Habib G, Bonnet JL, Vahanian A, Himbert D, et al. How should I treat refractory cardiogenic shock in a patient with chronic biventricular heart failure and mitral regurgitation with difficult valve characteristics? EuroIntervention. 2016;11:1201-1206. DOI: 10.4244/EIJV11I10A238
8. Bapat VV, Khaliel F, Ihleberg L. Delayed migration of Sapien valve following a transcatheter mitral valve-in-valve implantation. Catheter Cardiovasc Interv. 2014;83:E150-E154. DOI: 10.1002/ccd.25076

Cite this article as: Tandar A, Glotzbach JP, Welt FG, Sharma V, Browning K, Selzman CH, Saidi A, Bull DA. Successful First-in-Man Concomitant Transapical Transcatheter Aortic and Mitral Valve Replacements for Severe Native Aortic and Mitral Valve Stenosis Using the Edwards Certitude Delivery System. Structural Heart Disease. 2017;3(6):180-186. DOI: https://doi.org/10.12945/j.jshd.2017.026.17

Supplemental Media

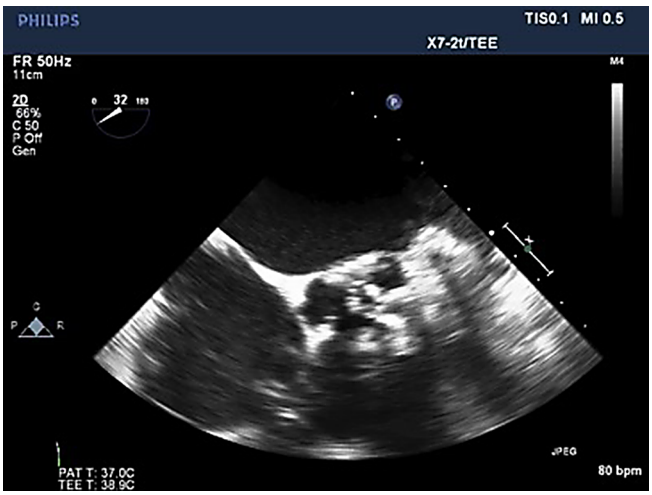

Video 1. Aortic valve pre-transcatheter aortic valve replacement. View supplemental video at https://doi.org/10.12945/j.jshd.2017.026.17.vid.01.

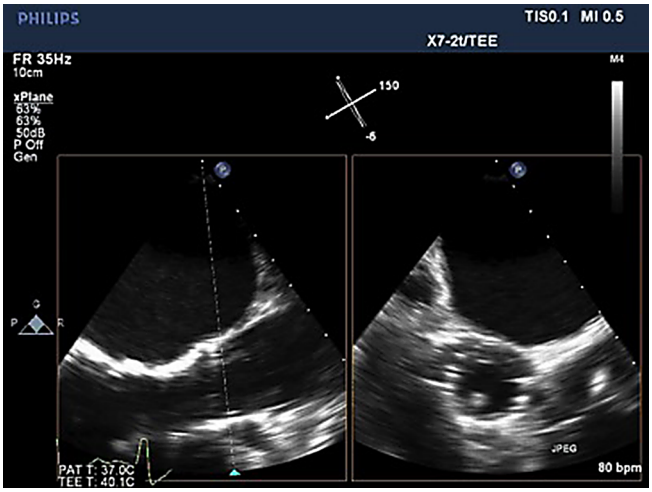

Video 2. Aortic valve post-transcatheter aortic valve replacement. View supplemental video at https://doi.org/10.12945/j.jshd.2017.026.17.vid.02.

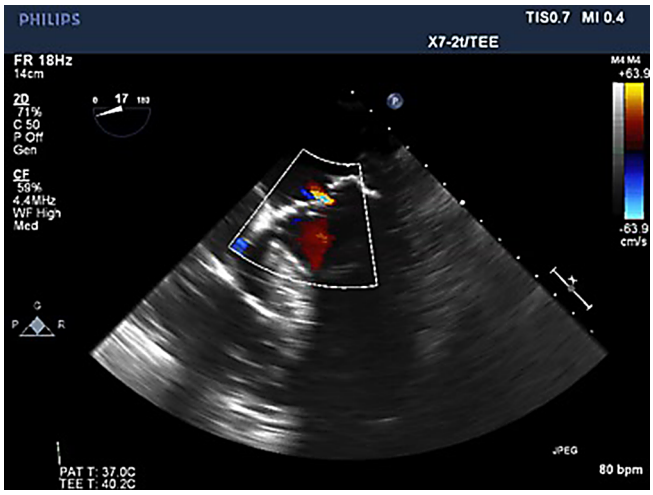

Video 3. Mitral stenosis pre-transcatheter mitral valve replacement. View supplemental video at https://doi.org/10.12945/j.jshd.2017.026.17.vid.03.

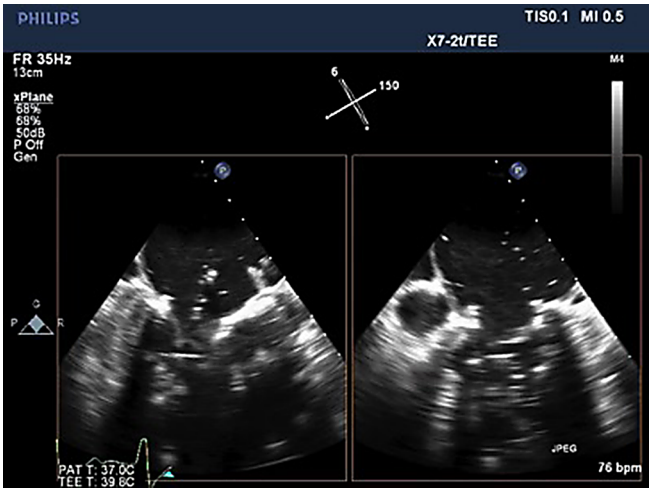

Video 4. Mitral valve post-transcatheter mitral valve replacement. View supplemental video at https://doi.org/10.12945/j.jshd.2017.026.17.vid.04.

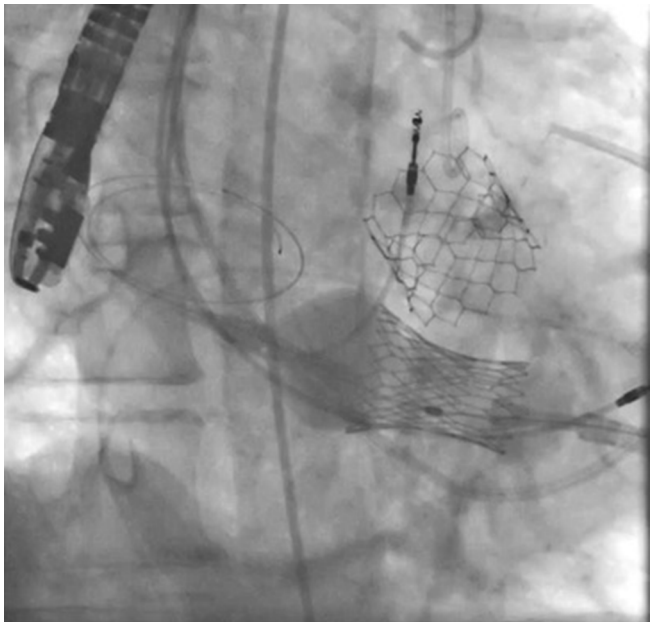

Video 5. Transapical transcatheter mitral valve replacement. View supplemental video at https://doi.org/10.12945/j.jshd.2017.026.17.vid.05.

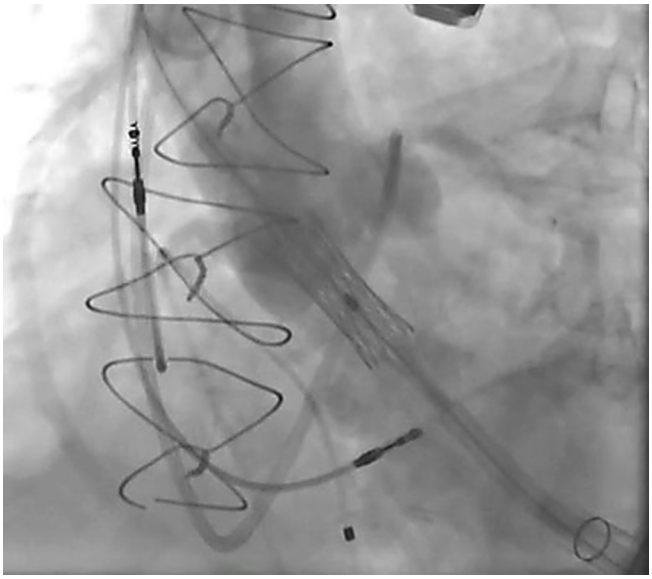

Video 6. Transapical transcatheter aortic valve replacement. View supplemental video at https://doi.org/10.12945/j.jshd.2017.026.17.vid.06.

JSHD
Journal of Structural Heart Disease

Case Report

Journal of Structural Heart Disease, December 2017, Volume 3, Issue 6:187-191
DOI: https://doi.org/10.12945/j.jshd.2017.022.17

Received: May 14, 2017
Accepted: May 29, 2017
Published online: December 2017

Improvement in Pulmonary Function After Closure of Atrial Septal Defect in a Patient With Cystic Fibrosis

Abdulfattah Saidi, MD[1*], Holly Carveth, MD[2], Anwar Tandar, MD[1]

[1] Division of Cardiovascular Medicine, University of Utah Hospital, Salt Lake City, Utah, United States

[2] Division of Pulmonary Medicine, University of Utah Hospital, Salt Lake City, Utah, United States

Abstract

Atrial septal defect (ASD) is a major cause of left-to-right intracardiac shunting. If persisting into adulthood, an ASD can lead to a larger shunt, which may eventually cause pulmonary hypertension and right ventricular failure. Large intracardiac shunts cannot be tolerated in patients with underlying lung disease such as cystic fibrosis. Although the association between an intracardiac shunt and cystic fibrosis has been reported in the literature, the impact of ASD closure on the clinical course of patients with cystic fibrosis has not been studied. Here, we report a case of ASD closure in a patient with cystic fibrosis with hypoxemia out of proportion to his lung disease. Closure of the ASD shunt resulted in significant improvement of his symptoms and pulmonary function testing.

Key Words

Atrial septal defect • Septal closure device • Cystic fibrosis

Introduction

Secundum atrial septal defect (ASD) is an isolated defect in the fossa ovalis between the atria. Although many ASDs close spontaneously during the first year after birth [1], the defect persists in some cases, causing a left-to-right shunt [2]. Left-to-right shunting, when significant, can cause dyspnea on exertion, which may not be well tolerated in patients with an underlying pulmonary condition such as cystic fibrosis. It is unknown whether ASD closure could lead to symptomatic improvement in these patients. Here, we report a case of ASD closure resulting in improved pulmonary function testing in a patient with cystic fibrosis with a bidirectional shunt and worsening functional capacity.

Case Presentation

Our patient was a 36-year-old man with cystic fibrosis diagnosed at birth with a dF508/dF508 genotype. His symptoms could be characterized as moderate airway disease complicated by chronic airway infections, pancreatic insufficiency, diabetes, and malnutrition. Progression of his clinical condition caused dyspnea with minimal exertion. He was referred to our cardiology service to be evaluated for hypoxemia out of proportion to his chronic pulmonary disease. Pulmonary function testing showed a forced expiratory volume in 1 s (FEV1) of 1.71 (43% predicted). Transesophageal echocardiography (TEE) showed a small ASD with a bidirectional shunt seen at rest (Figure 1). Right heart catheterization showed a pulmonary artery pressure of 26/7/16 mmHg and pulmonary vascular resistance of 1.7 Wood units. A decision was made to proceed with ASD closure, which

Fax +1 203 785 3346
E-Mail: jshd@scienceinternational.org
http://structuralheartdisease.org/

ISSN 2326-4004

Accessible online at:
http://structuralheartdisease.org/

* Corresponding Author:
Abdulfattah Saidi, MD
Division of Cardiovascular Medicine
University of Utah Hospital
50 North Medical Drive, Salt Lake City, UT 84132, USA
Tel. +801 585 5559; Fax: +801 581 7735; E-Mail: abdulfattah.saidi@hsc.utah.edu

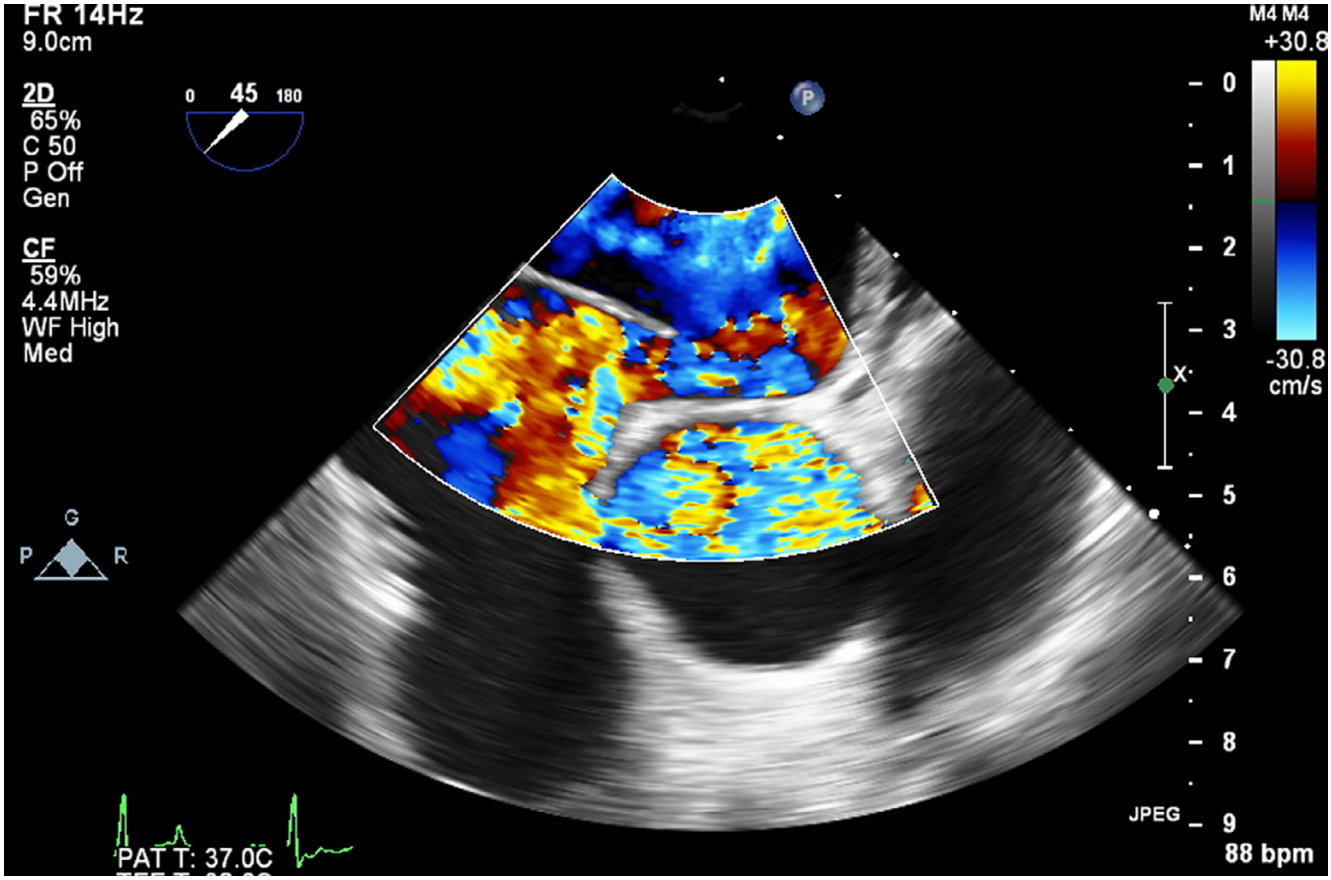

Figure 1. TEE showing bidirectional shunt before 20-mm Occluder Septal Helex placement.

was performed under the guidance of intra-cardiac echocardiography and fluoroscopy. A balloon sizing the defect was used, and the patient underwent ASD closure with a 25-mm Occluder Septal Helex. The indication for this closure was the presence of bidirectional flow that would ultimately lead to irreversible pulmonary hypertension. At the end of the procedure, an agitated saline study was performed, which revealed minimal residual shunt. Echocardiography performed the next day showed very minimal flow across the device as demonstrated by color Doppler. The patient was discharged to home on 81 mg aspirin and 75 mg clopidogrel daily for 3 months. He initially demonstrated symptomatic improvement with less oxygen requirement at rest. However, 3 months later, his symptoms of fatigue and dyspnea on exertion returned, and follow-up echocardiography demonstrated a large right-to-left intra-cardiac shunt at rest as demonstrated by an agitated saline study (Figure 2). His pulmonary function testing during this time showed an FEV1 of 1.78 (47% predicted). The patient was monitored for 1 year, during which his functional capacity and cystic fibrosis symptoms remained stable. He subsequently suffered from a neurological event suggestive of a transient ischemic attack of an embolic nature, after which he was considered for residual shunt closure. TEE revealed a deformity of the Helex device causing a bidirectional shunt via the inferior rim of the device. With further questioning, the patient admitted to using a high-frequency chest wall oscillation device a few days after his ASD closure as part of his routine treatment for cystic fibrosis.

The patient underwent closure of the residual shunt using a 30-mm Cardioform device. The second device was advanced across the defect and positioned to sandwich both sides of the previously placed Helex Occluder (Figure 3). The absence of a

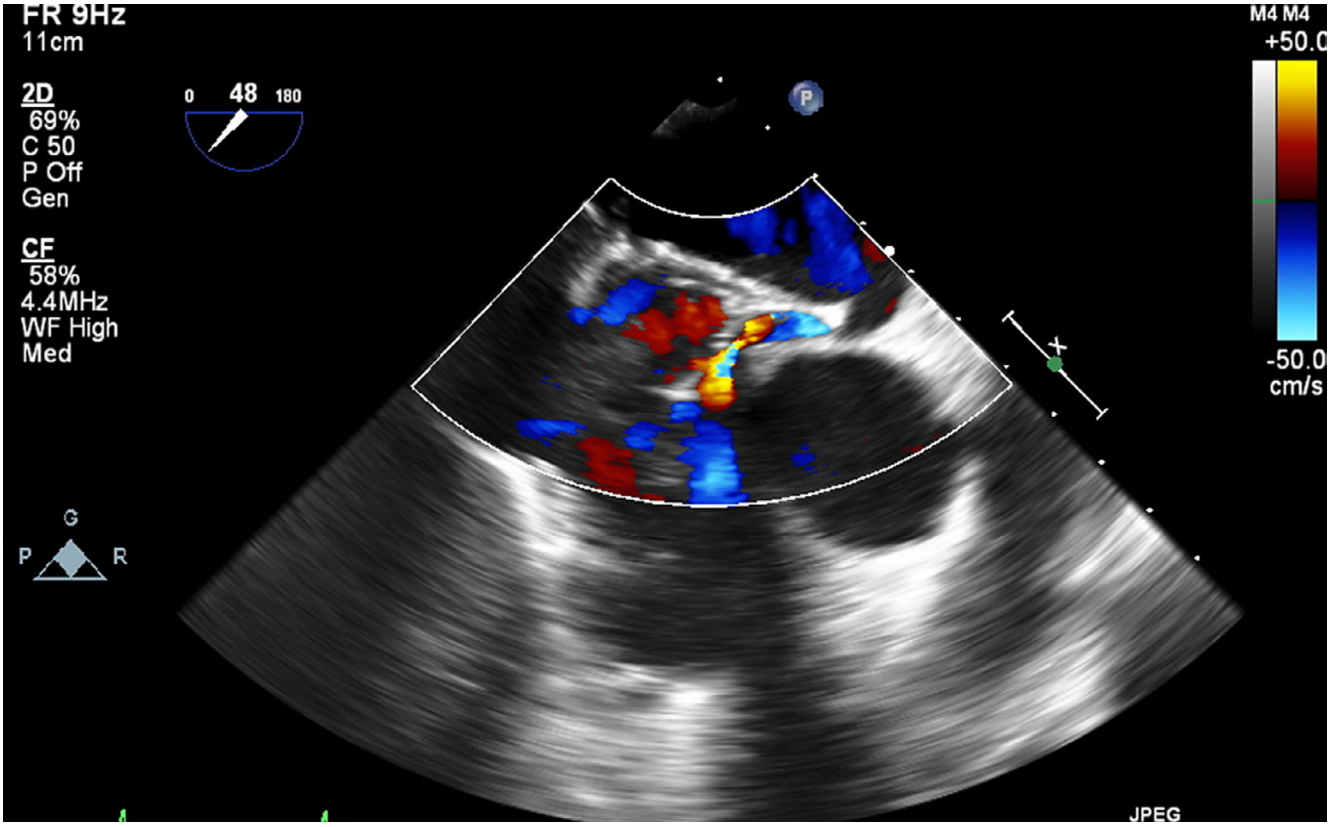

Figure 2. TEE showing residual shunt 1 year after 20-mm Occluder Septal Helex implantation.

residual shunt was confirmed with several negative agitated saline injections. He was advised to not use the high-frequency chest wall oscillation device for at least 12 months. At 6-month follow-up, the patient showed significant improvement in his functional capacity, with pulmonary function testing demonstrating a spike increase in FEV1 to 3.4 (89% predicted; Table 1).

Discussion

ASD is one of the most common adult congenital heart defects [3, 4]. It is caused by underdevelopment of the secundum septum or over-reabsorption of the primum septum. In most cases, ASDs close spontaneously during infancy [4, 5]; however, if persistent, their clinical impact is related to their location, size, and association with other defects [5, 6]. Small ASDs usually cause a left-to-right shunt without significant structural consequences in the right-sided heart chambers. However, larger ASDs, if not corrected in

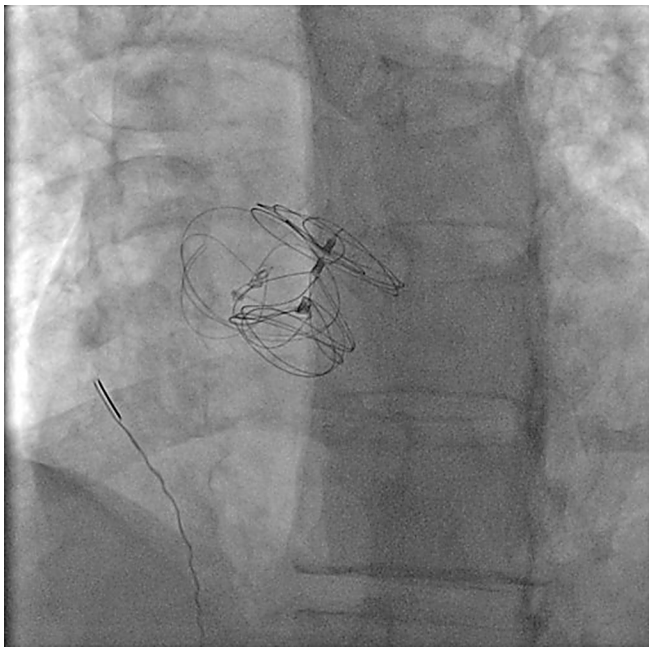

Figure 3. Fluoroscopy showing placement of a 30-mm Cardioform device adjacent to the previously placed 20-mm Occluder Septal Helex.

Table 1. Pulmonary function test of the patient over his clinical course.

	Before first ASD closure	After first ASD closure (with residual shunt)	*After second ASD closure (no significant residual shunt)*
FEV1	1.71 (43% predicted)	1.78 (47% predicted)	3.4 (89%predicted)
FEV1/FVC	53 (65% predicted)	61 (76% predicted)	76 (95% predicted)

early life, may lead to right-sided volume followed by pressure overload [6, 7], resulting in right atrial and ventricle enlargement and ultimately pulmonary vasculature remodeling and pulmonary hypertension with symptoms of right heart failure such as fatigue, decrease in functional capacity, and lung infections [7, 8]. The association between ASDs and cystic fibrosis is not well established. Two small series of patients with cystic fibrosis reported a 53–55% incidence of left-to-right shunt, mainly due to the presence of a patent foramen ovale (PFO) as seen by TEE [8, 9]. We can assume that patients with severe lung disease, such as cystic fibrosis in our case, will not tolerate hypoxemia caused by a significant right-to-left shunt. Current American College of Cardiology/American Heart Association guidelines [10] recommend percutaneous interventional therapy for ASDs in the presence of right atrial and right ventricle enlargement with or without symptoms before progressing to irreversible pulmonary hypertension, the presence of which is considered a contraindication for ASD closure. The impact of ASD closure on pulmonary function testing in patients with cystic fibrosis is not known. Belton et al. [11] reported a 29-year-old man with cystic fibrosis who underwent PFO closure after developing neurological symptoms. His pulmonary function had deteriorated at the time of the neurological event. Closure of his PFO improved his pulmonary function with an increase in FEV1 from 1.36 to 1.89 (33% to 47% predicted). The authors concluded that closure of the PFO may have had a significant impact on lung function. The indication for the first ASD closure in our case was the presence of bidirectional flow, for which we aimed to prevent the development of irreversible pulmonary hypertension that would preclude ASD closure. The first closure significantly improved pulmonary function testing before the device migrated and led to a residual shunt with worsening symptoms and test results. We assume that the use of a high-frequency chest wall oscillation device dislodged the initial occlude, resulting in larger residual shunt. The indication for the second closure was a neurological event caused by a paradoxical embolism. There was significant improvement in pulmonary function testing after the second ASD closure, which was not associated with a residual shunt immediately after the procedure.

In conclusion, percutaneous closure of ASD in patients with cystic fibrosis and hypoxemia out of proportion to their lung disease may improve pulmonary function testing and hypoxemia, although further studies are warranted to confirm this possibility.

Conflict of Interest

The authors have no conflict of interest relevant to this publication.

References

1. Hartmann AF, Elliott LP. Spontaneous physiological closure of atrial septal defect after infancy. Am J Cardiol. 1967;19:290-292. DOI: 10.1016/0002-9149(67)90549-8
2. Brassard M, Fouron JC, Van Doesburg NH, Mercier L, De Guise P. Outcome of children with atrial septal defect considered too small for surgical closure. Am J Cardiol. 1999;83:1552-1555. PMID: 10363870
3. Radzik D, Davignon A, Von Doesburg N, Fournier A, Marchand T, Ducharme G. Predictive factors for spontaneous closure of atrial septal defects diagnosed in the first 3 months of life. J Am Coll Cardiol. 1993;22:851-853. PMID: 8354823
4. Mcmahon CJ, Feltes TF, Fraley JK, Bricker JT, Gifka RG, Tortoriello TA, et al. Natural history of growth of secundum atrial septal defects and implications for transcatheter closure. Heart. 2002;87:256-259. PMID: 11847166
5. Hansilk A, Pospisil U, Salzer-Muhar U, Greber-Platzer S, Male C. Predictors of spontaneous closure of isolated secundum atrial septal defect in children: A longitudinal study. Pediatrics. 2006;118:1560-1565. DOI: 10.1542/peds.2005-3037

6. Granton JT, Rabinovitch M. Pulmonary arterial hypertension in congenital heart disease. Cardiol Clin. 2002;20:441-457. PMID: 12371012
7. Goetschmann S, Dibernardo S, Steinmann H, Pavlovic M, Sekarski N, Pfammatter, P. Frequency of severe pulmonary hypertension complicating "isolated" atrial septal defect in infancy. Am J Cardiol. 2008;102:340-342. DOI: 10.1016/j.amjcard.2008.03.061
8. Davidson A, Chandrasekaran K, Guida L, Holsclaw DS Jr. Enhancement of hypoxemia by atrial shunting in cystic fibrosis. Chest. 1990;98:543-545. PMID: 2394134
9. Espiritu JD, Kleinhenz ME. Patent foramen ovale is the most prevalent echocardiographic abnormality in adult cystic fibrosis. Am J Resp Crit Care Med. 2000;161:A71.
10. Warnes CA, Williams RG, Bashore TM, Child JS, Connolly HM, Dearani JA, et al. ACC/AHA 2008 guidelines for the management of adults with congenital heart disease: a report of the American College of Cardiology/American Heart Association Task Force on Practice Guidelines (Writing Committee to Develop Guidelines on the Management of Adults With Congenital Heart Disease). Developed in Collaboration With the American Society of Echocardiography, Heart Rhythm Society, International Society for Adult Congenital Heart Disease, Society for Cardiovascular Angiography and Interventions, and Society of Thoracic Surgeons. J Am Coll Cardiol. 2008;52:e143-e263. DOI: 10.1016/j.jacc.2008.10.001
11. Belton M, Gyi KM. Improvement in pulmonary function following closure of a patent foramen ovale in a man with cystic fibrosis. J R Soc Med. 2009;102:S59-S62. DOI: 10.1258/jrsm.2009.s19013

Cite this article as: Saidi A, Carveth H, Tandar A. Improvement in Pulmonary Function After Closure of Atrial Septal Defect in a Patient With Cystic Fibrosis. Structural Heart Disease. 2017;3(6):187-191. DOI: https://doi.org/10.12945/j.jshd.2017.022.17

JSHD
Journal of Structural Heart Disease

Case Report

Journal of Structural Heart Disease, December 2017, Volume 3, Issue 6:192-198
DOI: https://doi.org/10.12945/j.jshd.2017.033.17

Received: July 25, 2017
Accepted: August 07, 2017
Published online: December 2017

Worsening of Functional Mitral Regurgitation from Septal Dyssynchrony Induced by Ventricular Pacing in Ebstein's Anomaly Undergoing Percutaneous Mitral Valve Repair

Heajung L. Nguyen, MD[1*], Marcella A. Calfon Press, MD, PhD[2], Jamil A. Aboulhosn, MD[3], Jeannette P. Lin, MD[3], Peyman Benharash, MD[4], Eric H. Yang, MD[2]

[1] Department of Medicine, University of California at Los Angeles, Los Angeles, California, USA

[2] Division of Cardiology, Department of Medicine, University of California at Los Angeles, Los Angeles, California, USA

[3] Department of Medicine, Ahmanson-UCLA Adult Congenital Heart Disease Center, Los Angeles, California, USA

[4] Division of Cardiothoracic Surgery, Department of Surgery, University of California at Los Angeles, Los Angeles, California, USA

Abstract

A 67-year-old male with Ebstein's anomaly and a dual-chamber pacemaker due to sick sinus syndrome was admitted to our hospital with cardiogenic shock. Echocardiography revealed severe functional mitral valve regurgitation with preserved ejection fraction. He was referred for percutaneous mitral valve repair (PMVR) for refractory shock in the setting of prohibitive surgical risk. Invasive hemodynamics obtained during PMVR revealed worsening mitral regurgitation due to septal dyssynchrony induced by the patient's permanent pacing. He underwent successful PMVR with subsequent clinical recovery. Dyssynchrony from right ventricular apical pacing may exacerbate mitral regurgitation and heart failure. PMVR with MitraClip may be a safe and effective therapeutic option in patients with refractory cariogenic shock and severe mitral regurgitation.

Key Words

Mitral valve regurgitation • Dyssynchrony • Ventricular pacing • Percutaneous mitral valve repair • Ebstein's anomaly

Introduction

Percutaneous edge-to-edge mitral valve repair (PMVR) using the MitraClip (Abbott, Menlo Park, CA, USA) system is a novel method of reducing severe symptomatic degenerative mitral valve regurgitation (MR) in high-risk or inoperable patients. Although randomized trials for its use in functional MR and end-stage heart failure are currently underway, there are a few reported cases of its use as a rescue therapy in critically ill patients with refractory cardiogenic shock [1, 2]. Here, we present a case of cardiogenic shock in a patient with Ebstein's anomaly secondary to severe functional MR who underwent successful PMVR.

Case Presentation

A 67-year-old male with Ebstein's anomaly, history of bioprosthetic tricuspid valve replacement for tricuspid regurgitation, and dual-chamber pacemaker due to sick sinus syndrome presented to the emergency department with progressive dyspnea on exertion, abdominal distension, a 7-kg weight gain, and severe orthopnea. In the preceding 5 years, he had re-

Fax +1 203 785 3346
E-Mail: jshd@scienceinternational.org
http://structuralheartdisease.org/

ISSN 2326-4004

Accessible online at:
http://structuralheartdisease.org/

* Corresponding Author:
Heajung L. Nguyen, MD
Department of Medicine
University of California at Los Angeles
757 Westwood Plaza, Suite 7501, Los Angeles, CA 90095-7414, USA
Tel. +1 310 825 7375; Fax: +1 888 313 4815; E-Mail: HLnguyen@mednet.ucla.edu

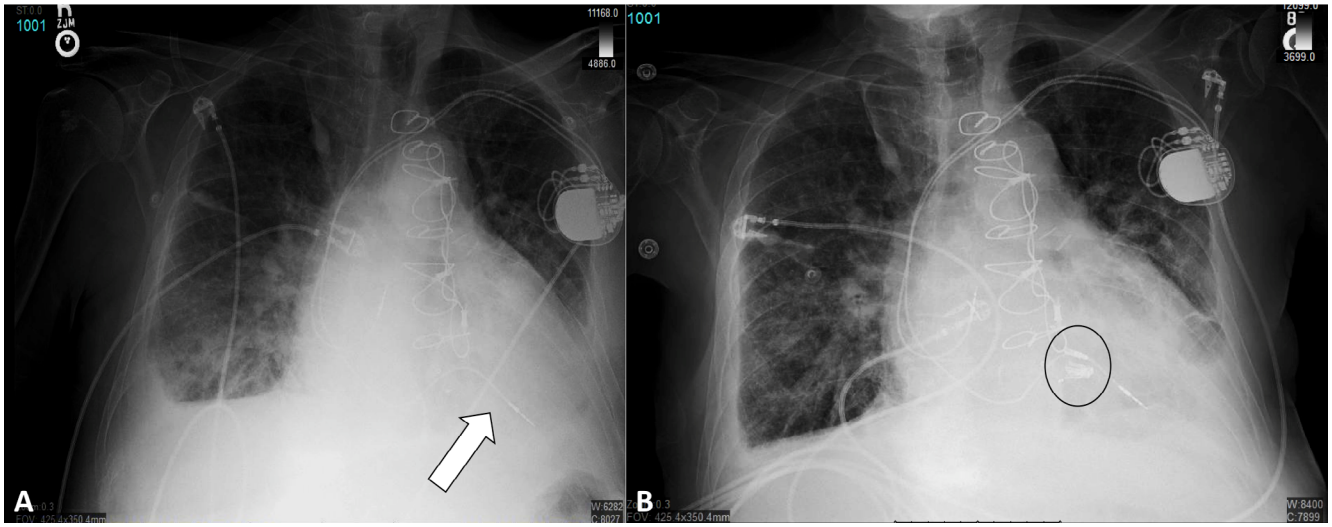

Figure 1. Portable chest radiographs throughout hospitalization. *Panel A.* Portable chest radiograph on admission demonstrating cardiomegaly with a dual-chamber pacemaker with the ventricular lead running on the outside of the bioprosthetic tricuspid valve (**arrow**), vascular congestion, pulmonary edema, and bilateral pleural effusions. *Panel B.* Portable chest radiograph on hospital day 12 (post-mitral valve repair day 6) showing stable placement of three MitraClips (**circle**) and improving pulmonary edema.

quired multiple hospitalizations for dyspnea, weight gain, and abdominal distension despite escalating doses of diuretics.

On physical examination, he was severely dyspneic with an oxygen saturation of 95% on non-invasive bi-level positive pressure ventilation. His blood pressure was 96/67 mmHg with an atrioventricular paced heart rate of 80 beats per minute. His physical examination was notable for significant jugular venous distension, a grade II/VI holosystolic murmur heard loudest at the apex, bibasilar crackles, abdominal distension, and 1+ bilateral lower extremity edema. Serum brain natriuretic peptide was elevated at 364 pg/mL, and chest radiography showed enlargement of the cardiac silhouette, vascular congestion, pulmonary edema, and bilateral pleural effusions (Figure 1A).

Table 1. Invasive hemodynamics immediately before and after percutaneous mitral valve repair. Note all hemodynamics were measured on the same dosages of dopamine, dobutamine, and epinephrine.

	Pre-Mitral Valve Repair	Post-Mitral Valve Repair
Mean Right Atrial Pressure (mmHg)	23	17
Pulmonary Artery Pressure (mmHg)	67/30	60/27
Pulmonary Capillary Wedge Pressure (mmHg)	27	18
Left Atrial Pressure, a/v waves (mmHg)	18/65	14/30
Cardiac Output (L/min; via thermodilution)	6.1	7.1
Cardiac Index (L/min/m2; via thermodilution)	3.2	3.8

Transthoracic and transesophageal echocardiography revealed severe MR, severe biatrial enlargement, and preserved left ventricular ejection fraction with left ventricular end-diastolic and end-systolic dimensions of 52 mm and 40 mm, respectively (Figure 2A and 2B, Video 1 and 2). Tenting of the mitral leaflets with poor coaptation of anterior and posterior leaflets was noted, consistent with functional MR. The bioprosthetic tricuspid valve appeared to function normally. Within 24 h of admission, he quickly progressed to cardiogenic shock requiring dobutamine and dopamine , and progressive anuric renal failure requiring continuous renal replacement therapy. He was evaluated for PMVR with via MitraClip given prohibitive surgical risk with 30-day Society of Thoracic Surgeons predictive operative mortality risk scores of 43% and 36% for mitral valve replacement and repair, respectively.

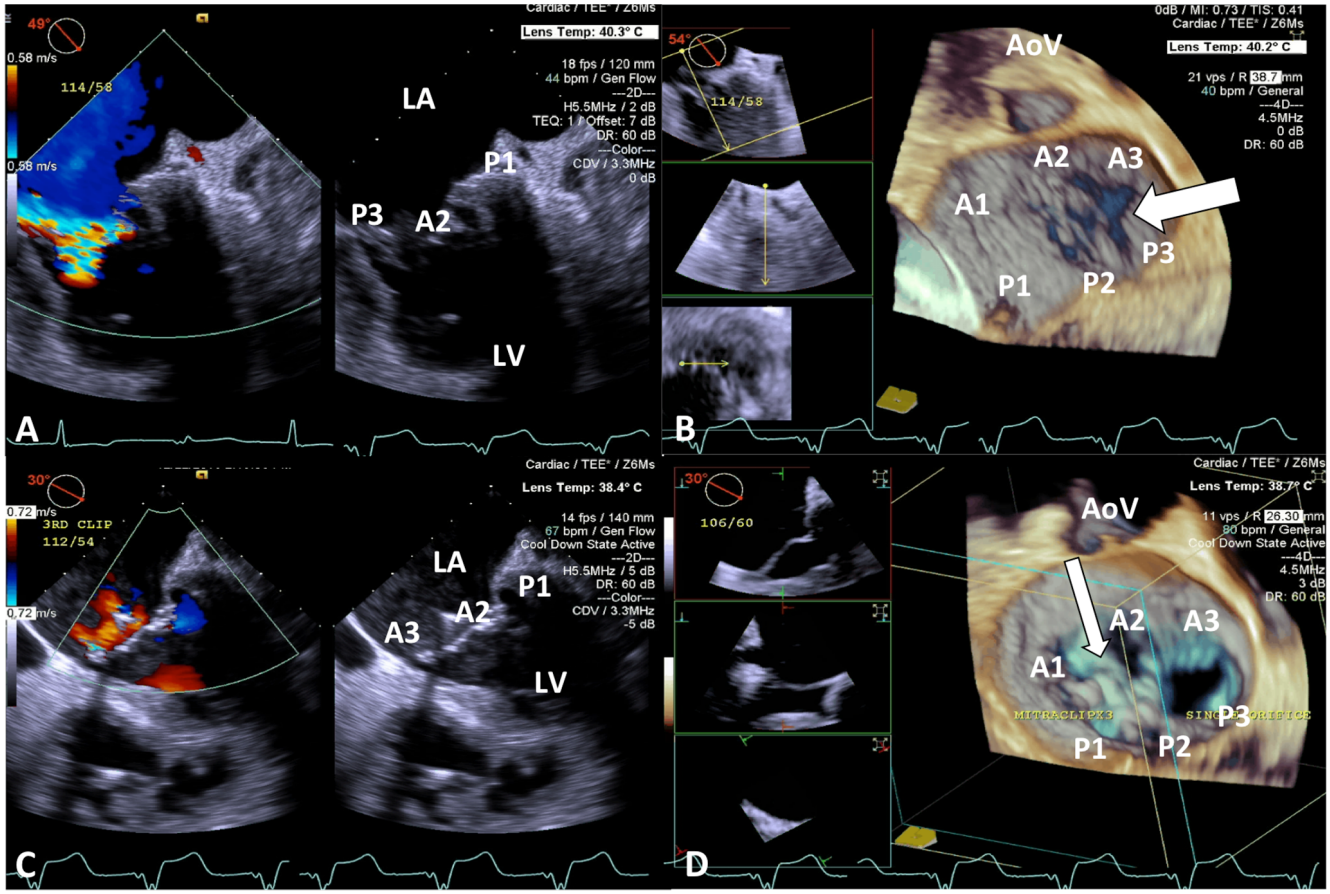

Figure 2. Transesophageal echocardiography before and after percutaneous mitral valve repair. *Panel A.* Two-dimensional midesophageal 50° view of the mitral valve with color doppler (**left panel**) showing an approximate commissural view of the P3, A2, and P1 scallops. Severe MR is noted, with a broad base due to leaflet malcoaptation resulting in a functional etiology from atrial dilation. *Panel B.* Three-dimensional live visualization of the mitral valve from the view of the left atrium. Three-dimensional imaging allows

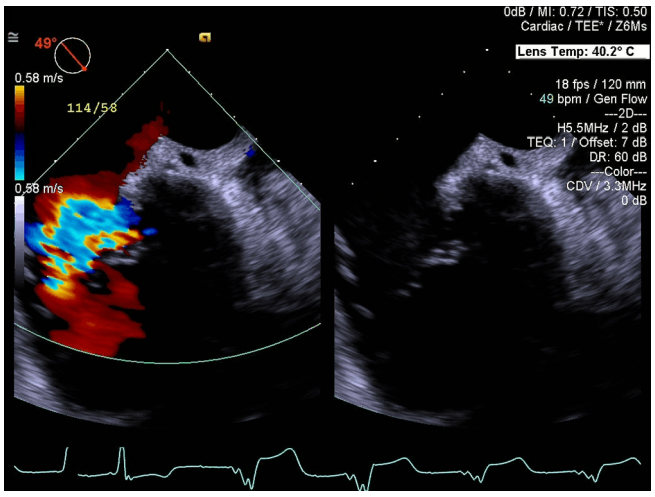

Video 1. Two-dimensional transesophageal echocardiography of the mitral valve as seen in Figure 2A before percutaneous mitral valve repair. View supplemental video at https://doi.org/10.12945/j.jshd.2017.033.17.vid.01.

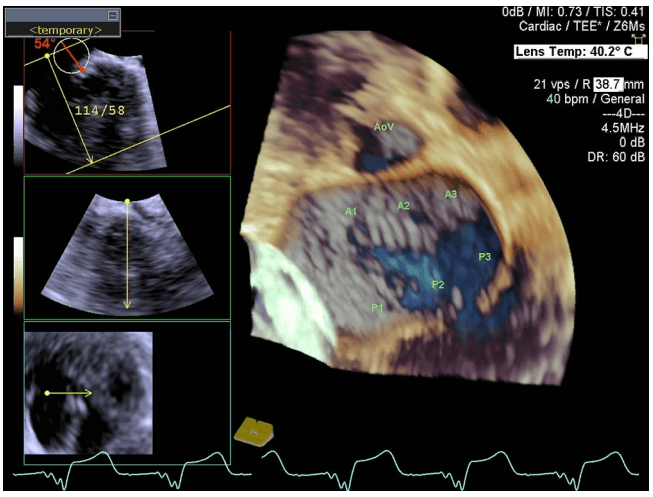

Video 2. Three-dimensional transesophageal echocardiography of the mitral valve as seen in Figure 2B before percutaneous mitral valve repair. View supplemental video at https://doi.org/10.12945/j.jshd.2017.033.17.vid.02.

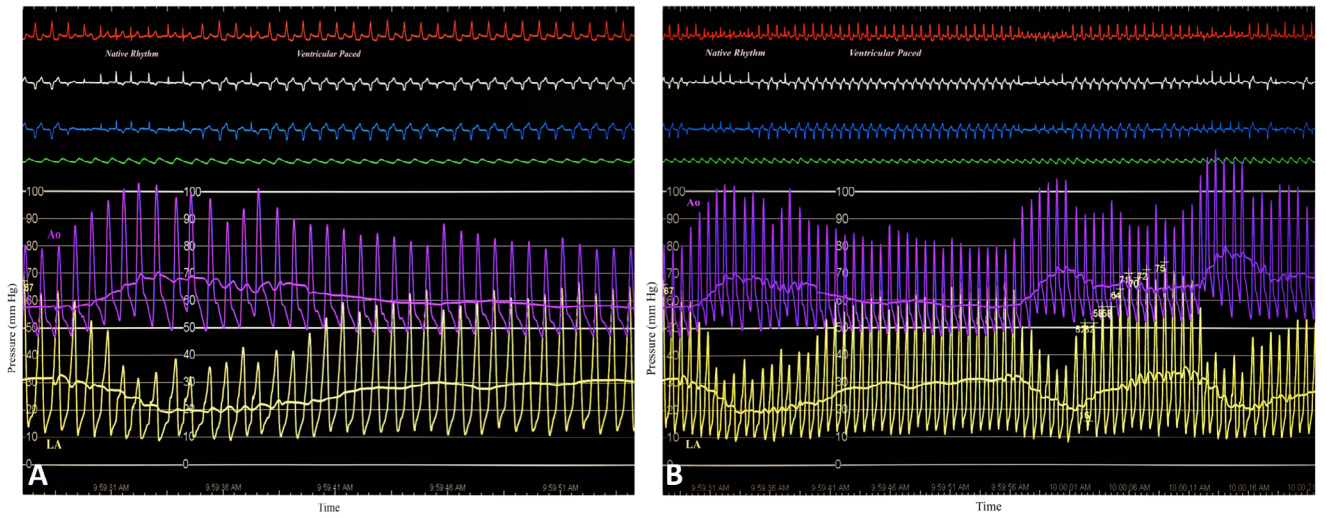

Figure 3. Invasive cardiac hemodynamics measuring simultaneous aortic (**purple**) and left atrial (**yellow**) waveforms before mitral valve repair. When the patient was in a ventricular paced rhythm, increased left atrial pressures with a mean of 30 mmHg with prominent V waves of up to 75 mmHg were noted. Simultaneous central aortic pressures decreased with ventricular pacing (mean 58 mmHg). Native ventricular conduction was associated with decreased left atrial pressures (mean 20 mmHg) with smaller V waves and enhanced arterial pressures (mean 68 mmHg). Ao = aortic pressures; LA = left atrial pressure.

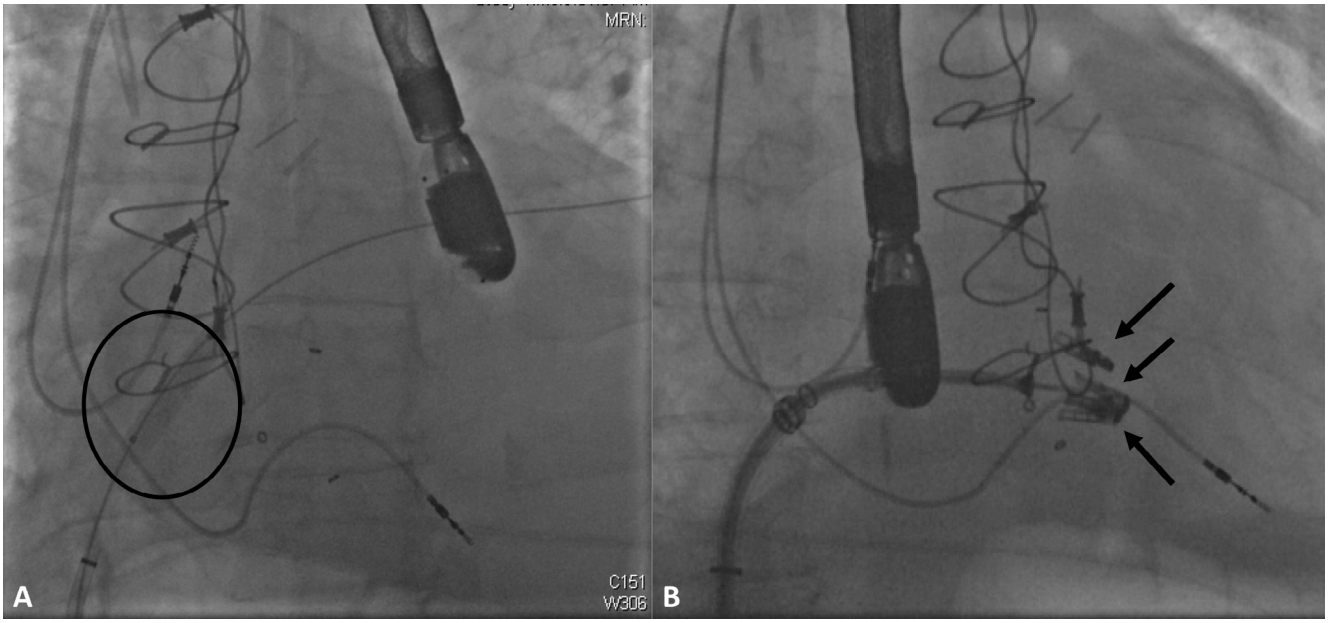

Figure 4. Intraprocedural fluoroscopy, anteroposterior view, during MitraClip procedure. *Panel A*. Fluoroscopy performed after transseptal puncture. Balloon dilation (**circle**) of the interatrial septum was performed to allow for passage of the MitraClip delivery catheter. *Panel B*. Fluoroscopy visualizing the placement of three MitraClips (**arrows**).

Intraoperative pre-repair hemodynamics revealed two distinct left atrial and arterial waveforms depending on the patient's cardiac rhythm, illustrating its electromechanical influence on MR (Figure 3). Whereas the patient was predominantly atrioventricular (AV) paced, a drop in V waves and concurrent rise in aortic waveforms was observed when the patient had native AV conduction. In comparison, resumption of

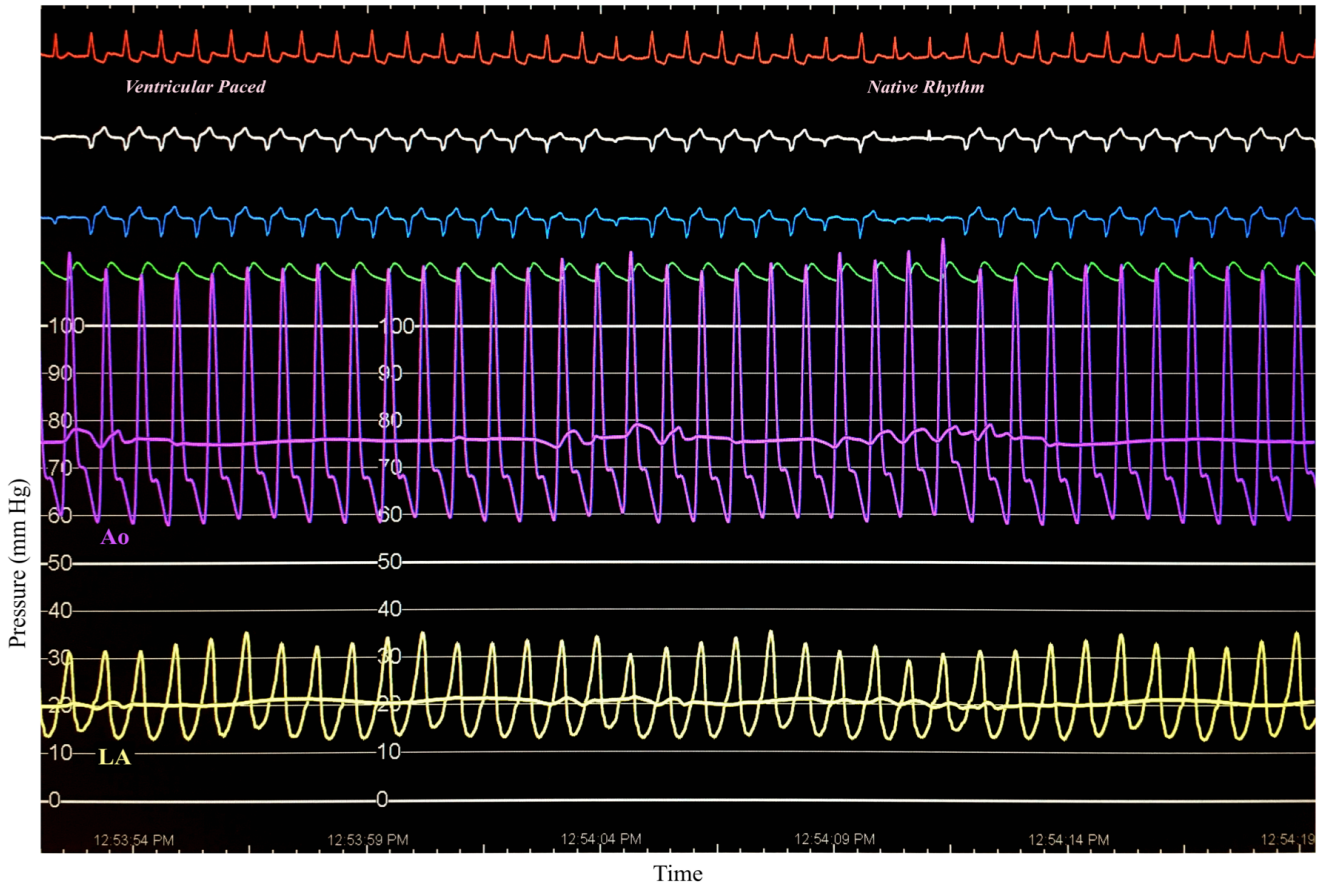

Figure 5. Cardiac invasive hemodynamics after mitral valve repair with measurement of aortic (**purple**) and left atrial (**yellow**) pressures. After MitraClip placement, overall improved left atrial pressures (mean 20 mm Hg with V waves up to 33 mm Hg) and arterial pressures (mean 76 mm Hg) are seen with no significant pressure changes during ventricular paced or native conducted rhythms. Of note, minimal pressure variations did not correlate with the patient's ventilatory changes.

right ventricular (RV) pacing resulted in a marked elevation of V waves (up to 67 mmHg) and decrease in aortic pressures, demonstrating worsening of MR.

The patient underwent successful PMVR with deployment of three MitraClips along the A1-2/P1-2 interface, with reduction of MR from severe to mild and a mean transmitral gradient of 3 mmHg (three-dimensional planimetry valve orifice area of 3.6 cm^2) (Figure 2B, 2C, and 4, Video 3 and 4). Post-MitraClip hemodynamics confirmed dramatic improvement in left atrial pressures throughout both paced and native rhythms (Figure 5, Table 1). Transthoracic echocardiography on postoperative day 1 showed a mild decrease in left ventricular size and modest drop in left ventricular ejection fraction from 60–65% to 45–50% but with sustained mild residual MR.

Postoperatively, the patient was rapidly weaned off vasopressor support with recovery of renal function (Figure 1B). He was discharged 10 days after the procedure, with plans for pacemaker upgrade to cardiac resynchronization therapy. One month post-procedure, he was doing well, with New York Heart Association class II symptoms and maintenance of a stable weight on an oral diuretic regimen with brain natriuretic peptide of 126 pg/mL. Follow-up echocardiography confirmed no significant changes, with stable mild residual MR.

Discussion

Cardiac pacing is an established and effective treatment for a variety of bradyarrhythmias. Although the

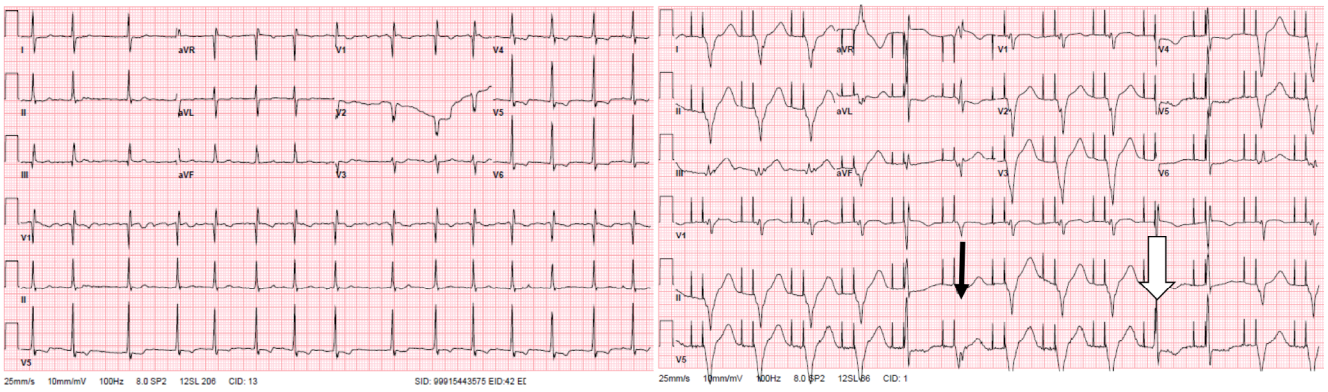

Figure 6. Twelve-lead electrocardiograms. *Panel A*. Electrocardiogram prior to pacemaker placement, demonstrating atrial fibrillation with an incomplete right bundle branch block pattern, with normal axis and nonspecific ST-T segment abnormalities seen inferolaterally. *Panel B*. Electrocardiogram after dual-chamber pacemaker placement, demonstrating an atrioventricular paced rhythm and a paced ventricular morphology with an indeterminate axis and atypical left bundle branch morphology (no broad R waves noted in lateral leads). Pseudofusion (**thick arrow**) was intermittently noted, revealing the patient's native QRS morphology and fusion (**thin arrow**).

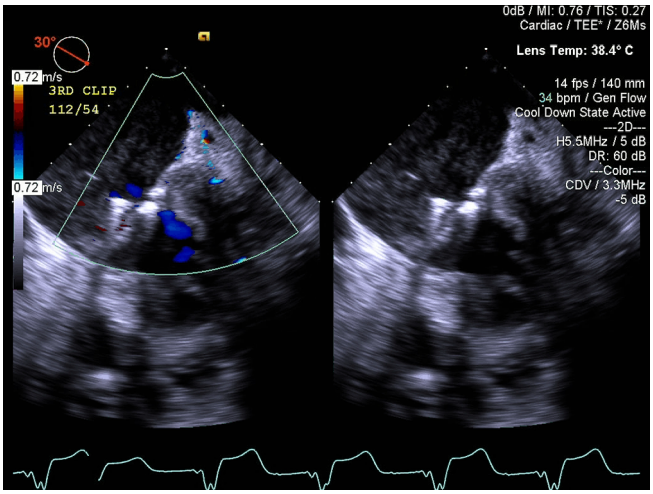

Video 3. Two-dimensional transesophageal echocardiography of the mitral valve as seen in Figure 2C after percutaneous mitral valve repair. View supplemental video at https://doi.org/10.12945/j.jshd.2017.033.17.vid.03.

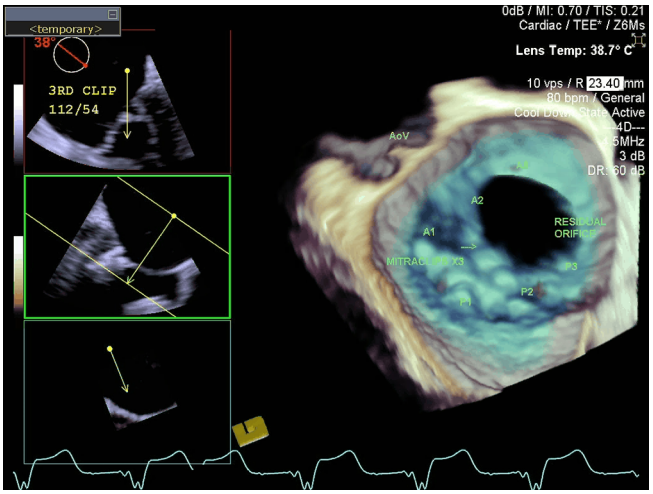

Video 4. Three-dimensional transesophageal echocardiography of the mitral valve as seen in Figure 2D after percutaneous mitral valve repair. View supplemental video at https://doi.org/10.12945/j.jshd.2017.033.17.vid.04.

right ventricular apex is the standard pacing site for dual-chamber pacemakers, several studies report detrimental effects of electrical dyssynchrony from RV pacing, including exacerbation of valvular dysfunction and heart failure [3, 4].

In this case, invasive hemodynamics obtained during PMVR demonstrated worsening of functional MR from septal dyssynchrony induced by RV apical pacing. The association between MR and right ventricular apical pacing has been described in many clinical scenarios ranging from acute severe MR immediately following pacemaker implantation to slow progression of MR in the setting of chronic right ventricular apical pacing [4-6].

The mechanism of MR with RV pacing is derived from intraventricular dyssynchrony. Pacing from the right ventricular apex induces an iatrogenic form of left bundle branch block as depolarization spreads from the apex to the base, as demonstrated by the patient's electrocardiograms before and after du-

al-chamber pacemaker placement (Figure 6). This abnormal left ventricular activation sequence causes delayed reduction of both the mitral annular size and regurgitant orifice size, leading to abnormal leaflet coaptation and enhanced MR [7].

Moreover, a hallmark of Ebstein's anomaly is dyssynchrony of the basal septum at the attachment site of the septal leaflet [8]. Although the patient had previously undergone surgical tricuspid valve replacement, residual septal dyskinesis may have also further contributed to worsened MR.

This case highlights the hemodynamic effects of right ventricular pacing in MR and demonstrates the potential utility of the MitraClip system as a feasible and effective salvage therapy option in refractory cardiogenic shock. Further experience and research is needed to clarify which patients can be hemodynamically significantly affected by right ventricular pacing.

Conflict of Interest

The authors have no conflict of interest relevant to this publication.

Comment on this Article or Ask a Question

References

1. Zuern CS, Schreieck J, Weig HJ, Gawaz M, May AE. Percutaneous mitral valve repair using the MitraClip in acute cardiogenic shock. Clin Res Cardiol. 2011;100:719-721. DOI: 10.1007/s00392-011-0324-1
2. Pleger ST, Chorianopoulos E, Krumsdorf U, Katus HA, Bekeredjian R. Percutaneous edge-to-edge repair of mitral regurgitation as a bail-out strategy in critically ill patients. J Invasive Cardiol. 2013;25:69-72. PMID: 23388223
3. Cannan CR, Higano ST, Holmes DR Jr. Pacemaker induced mitral regurgitation: an alternative form of pacemaker syndrome. Pacing Clin Electrophysiol. 1997;20:735-738. PMID: 09080503
4. Wong DT, Leong DP, Khurana S, Puri R, Tayeb H, Sanders P. Severe mitral regurgitation due to right ventricular apical pacing. BMJ Case Reports. 2010;pii:bcr1220092524. DOI: 10.1136/bcr.12.2009.2524
5. Miranda R, Almeida S, Brandão L, Alvarenga C, Ribeiro L, Almeida AR, et al. Acute severe mitral regurgitation as an early complication of pacemaker implantation. Europace. 2010;12:1791-1792. DOI: 10.1093/europace/euq191
6. Alizadeh A, Sanati HR, Haji-Karimi M, Yazdi AH, Rad MA, Haghjoo M, et al. Induction and aggravation of atrioventricular valve regurgitation in the course of chronic right ventricular apical pacing. Europace. 2011;13:1587-1590. DOI: 10.1093/europace/eur198
7. Ebrille E, DeSimone CV, Vaidya VR, Chahal AA, Nkomo VT, Asirvatham SJ. Ventricular pacing – Electromechanical consequences and valvular function. Indian Pacing Electrophysiol J. 2016;16:19-30. DOI: 10.1016/j.ipej.2016.02.013
8. Méndez C, Soler R, Rodriguez E, López M, Alvarez L, Fernández N, et al. Magnetic resonance imaging of abnormal ventricular septal motion in heart diseases: A pictorial review. Insights Imaging. 2011;2:483-492. DOI: https://doi.org/10.1007/s13244-011-0093-4

Cite this article as: Nguyen HL, Calfon Press MA, Aboulhosn JA, Lin JP, Benharash P, Yang EH. Worsening of Functional Mitral Regurgitation from Septal Dyssynchrony Induced by Ventricular Pacing in Ebstein's Anomaly Undergoing Percutaneous Mitral Valve Repair. Structural Heart Disease. 2017;3(6):192-198. DOI: https://doi.org/10.12945/j.jshd.2017.033.17